

# High-Dimensional Time-Varying Coefficient Estimation in Diffusion Models

Donggyu Kim<sup>a\*</sup>, Minseog Oh<sup>b</sup>, and Minseok Shin<sup>b</sup>

<sup>a</sup>University of California, Riverside

<sup>b</sup>Pohang University of Science and Technology (POSTECH)

September 25, 2025

## Abstract

In this paper, we develop a novel high-dimensional time-varying coefficient estimation method, based on high-dimensional Itô diffusion processes. To account for high-dimensional time-varying coefficients, we first estimate local (or instantaneous) coefficients using a time-localized Dantzig selection scheme under a sparsity condition, which results in biased local coefficient estimators due to the regularization. To handle the bias, we propose a debiasing scheme, which provides well-performing unbiased local coefficient estimators. With the unbiased local coefficient estimators, we estimate the integrated coefficient, and to further account for the sparsity of the coefficient process, we apply thresholding schemes. We call this Thresholding dEbiased Dantzig (TED). We establish asymptotic properties of the proposed TED estimator. In the empirical analysis, we apply the TED procedure to analyzing high-dimensional factor models using high-frequency data.

**Keywords:** Dantzig selection, debiased, diffusion process, factor model, sparsity

---

\*Corresponding author. E-mail address: donggyu.kim@ucr.edu.

# 1 Introduction

To explain various data types, numerous regression-based models have been developed. Especially, advances in technology provide us big data, which causes the curse of dimensionality problem. To tackle this problem in the high-dimensional regression, we usually assume the sparsity of variables, that is, the number of significant coefficients is small. To accommodate the sparsity condition, we often employ the LASSO procedure (Tibshirani, 1996), SCAD (Fan and Li, 2001), and Dantzig selector (Candes and Tao, 2007). The works of Belloni et al. (2014); Feng et al. (2020); Yuan and Lin (2006); Zou (2006) are useful for further reading. There are numerous related papers that can be found in the above literature. These estimation methods result in sparse coefficients, and under the sparsity condition, they are consistent estimators (Negahban et al., 2012). Under the diffusion process, Ciolek et al. (2022) studied the properties of the LASSO estimator of the drift component and Gaïffas and Matulewicz (2019) proposed the estimation procedure for the drift parameter in the high-dimensional Ornstein–Uhlenbeck (OU) process.

On the other hand, in high-frequency finance, we often observe that coefficients in the regression model are time-varying. For example, Andersen et al. (2021) investigated the intraday variation of the local coefficients, which are called the market betas, between the individual assets and market index. To account for the time-varying feature, Mykland and Zhang (2009) computed the market beta as the aggregation of the market betas estimated over local blocks. To evaluate the coefficients of multi factor models, Aït-Sahalia et al. (2020) proposed an integrated coefficient approach using the local coefficient. See also Chen (2018); Oh et al. (2024). We call this high-frequency regression. Recently, Chen et al. (2024) proposed the high-dimensional market beta estimation procedure with large dependent variables and almost finite common factors. However, in the field of finance, there are hundreds of potential factor candidates that explain the cross section of expected stock returns (Cochrane, 2011; Harvey et al., 2016; Hou et al., 2020; McLean and Pontiff, 2016). Thus, we also en-

counter the curse of dimensionality in high-frequency regressions, so the estimation methods developed for the finite dimension fail to estimate the coefficients consistently. To overcome this issue, we can consider the high-dimensional regression methods such as the LASSO (Tibshirani, 1996), Dantzig selector (Candes and Tao, 2007), and SCAD (Fan and Li, 2001). However, the direct application of these methods cannot explain the time-varying feature of the coefficient process and may suffer from the model errors. Thus, to fully benefit from the utilization of high-frequency financial data in the high-dimensional regression, we need to develop methodologies that can handle both the curse of dimensionality as well as the time-varying coefficients.

In this paper, we introduce a novel high-dimensional high-frequency regression estimation procedure which can accommodate the sparse and time-varying coefficient processes. To model the high-frequency data, we employ diffusion processes whose stochastic difference equations have a time series regression structure. We also assume that the coefficient process  $\beta_t$  follows a diffusion process. In this paper, the parameter of interest is the integrated coefficient,  $\int_0^1 \beta_t dt$ , that represents the average relationship between variables. To handle the curse of dimensionality, we assume that the coefficient processes are sparse, and to account for the sparsity of the time-varying coefficient process, we employ the Dantzig selector procedure (Candes and Tao, 2007). Specifically, due to the time-varying phenomena, we cannot estimate the integrated coefficient directly, and so we first estimate the instantaneous (or local) coefficients using the time-localized Dantzig selector procedure, based on the definition of  $\beta_t$ . Alternatively, a LASSO-type estimator can be used instead of the Dantzig selector, as demonstrated in Shin and Kim (2023), who builds on this study by incorporating robustness against heavy-tailed data distributions. It is worth mentioning that Shin and Kim (2023) wrote the paper based on the estimation structure of our paper, and their main contribution is to handle heavy-tailed distribution and to extend the estimation structure to the LASSO-type. Then, to mitigate the bias coming from the regularization of the Dantzig selector,

we propose a debiasing scheme and estimate the integrated coefficient with the debiased Dantzig instantaneous coefficients. With the debiasing scheme, we can obtain more accurate estimators in terms of the element-wise convergence rate; however, the estimated integrated coefficient is not sparse. Thus, to accommodate the sparsity, we further regularize the estimated integrated coefficient. We call this Thresholding dEbiased Dantzig (TED). To our best knowledge, this is the first paper that handles a high-dimensional integrated time-varying coefficient based on high-frequency data. We also establish its asymptotic properties.

The rest of paper is organized as follows. Section 2 introduces the model set-up. Section 3 proposes the TED estimation procedure and establishes its asymptotic properties. In Section 4, we conduct a simulation study to check the finite sample performance of the TED estimation procedure, and in Section 5, we apply the TED to the high-frequency financial data. The conclusion is presented in Section 6, and we collect all of the proofs and supplementary materials in Appendix.

## 2 The model set-up

We consider the following non-parametric time series regression diffusion model:

$$dY_t = \boldsymbol{\beta}_t^\top d\mathbf{X}_t + dZ_t, \quad (2.1)$$

where  $Y_t$  is a dependent process,  $\mathbf{X}_t$  is a  $p$ -dimensional multivariate covariate process,  $\boldsymbol{\beta}_t$  is a coefficient process, and  $Z_t$  is a residual process. The  $p$ -dimensional covariate process  $\mathbf{X}_t$  and residual process  $Z_t$  satisfy

$$d\mathbf{X}_t = \boldsymbol{\mu}_t dt + \boldsymbol{\sigma}_t d\mathbf{B}_t \quad \text{and} \quad dZ_t = \nu_t dW_t, \quad (2.2)$$

where  $\boldsymbol{\mu}_t$  is a drift process,  $\boldsymbol{\sigma}_t$  and  $\nu_t$  are instantaneous volatility processes,  $\mathbf{B}_t$  and  $W_t$  are  $p$ -dimensional and one-dimensional standard Brownian motions, respectively, and  $\mathbf{B}_t$  and  $W_t$  are independent. The stochastic processes  $\boldsymbol{\mu}_t$ ,  $\boldsymbol{\beta}_t$ ,  $\boldsymbol{\sigma}_t$ , and  $\nu_t$  are predictable. To account for the time-varying coefficient, we further assume that the coefficient  $\boldsymbol{\beta}_t$  satisfies the following diffusion process:

$$d\boldsymbol{\beta}_t = \boldsymbol{\mu}_{\boldsymbol{\beta},t}dt + \boldsymbol{\nu}_{\boldsymbol{\beta},t}d\mathbf{W}_t^\beta, \quad (2.3)$$

where  $\boldsymbol{\mu}_{\boldsymbol{\beta},t}$  and  $\boldsymbol{\nu}_{\boldsymbol{\beta},t}$  are predictable, and  $\mathbf{W}_t^\beta$  is  $p$ -dimensional standard Brownian motion. We do not impose any restriction on the dependence structure between  $\mathbf{W}_t^\beta$  and  $(\mathbf{B}_t, W_t)$ , while we assume independence between  $\mathbf{B}_t$  and  $W_t$  for identification. We note that (2.3) includes many continuous-time models commonly used in economics and finance, including mean-reverting processes such as the OU process. Since the drift and volatility terms are modeled as general predictable stochastic processes, they can incorporate various forms of endogeneity. To figure out the average relationship between the covariate and dependent processes, we consider the integrated coefficient:

$$I\boldsymbol{\beta} = (I\beta_i)_{i=1,\dots,p} = \int_0^1 \boldsymbol{\beta}_t dt.$$

In finance, hundreds of potential factor candidates have been proposed in order to explain the cross section of expected stock returns (Cochrane, 2011; Harvey et al., 2016; Hou et al., 2020; McLean and Pontiff, 2016). That is, the dimensionality,  $p$ , of the covariate process is large. Thus, we often run into the curse of dimensionality problem when handling financial data. However, all of them may not be significant; thus, to account for this, we assume that the coefficient process  $\boldsymbol{\beta}_t = (\beta_{1t}, \dots, \beta_{pt})^\top$  satisfies the following weak sparsity condition as defined in Fan et al. (2017):

$$\sup_{0 \leq t \leq 1} \sum_{i=1}^p |\beta_{it}|^\delta \leq s_p \quad \text{and} \quad \sum_{i=1}^p |I\beta_i|^\delta \leq s_p \quad \text{a.s.}, \quad (2.4)$$

where  $0^0$  is defined as 0,  $\delta \in [0, 1)$ , and  $s_p$  is diverging slowly with respect to  $p$ , for example,  $\log p$ . See also Bickel and Levina (2008); Cai and Liu (2011); Cai et al. (2011); Cai and Zhou (2012). In practice, it is often convenient to assume  $\delta = 0$ , which corresponds to the exact sparsity condition with only a few nonzero coefficients. In this paper, we investigate asymptotic properties under the more general sparsity condition, which includes the above exact sparsity condition as a special case. This sparsity assumption reflects that not all covariates have strong effects on the dependent process; otherwise, the volatility of the dependent process would diverge. We note that with the randomness of the coefficient process, in general, the sparsity condition (2.4) is satisfied with high probability. However, for simplicity, we assume that the sparsity condition is satisfied almost surely. The sparsity condition is also widely employed in the high-frequency finance literature (Ciolek et al., 2022; Gaïffas and Matulewicz, 2019; Kim et al., 2016, 2018; Tao et al., 2013; Wang and Zou, 2010). To ensure that the diffusion process satisfies the sparsity condition, additional conditions on  $\boldsymbol{\mu}_{\beta,t}$  and  $\boldsymbol{\nu}_{\beta,t}$  should be imposed. One sufficient condition is that there exists a set of indices  $S$  such that  $|S| \leq s_p$  and  $\boldsymbol{\mu}_{\beta,t,i} = \boldsymbol{\nu}_{\beta,t,j,k} = 0$  for all  $i \notin S$ ,  $(j, k) \notin \{(i, i) : i \in S\}$ , and  $t \in [0, 1]$ . There might be more general sufficient conditions, such as those allowing for time-varying exact sparsity patterns, but we leave exploring such conditions for a future study.

### 3 High-dimensional high-frequency regression

#### 3.1 Estimation procedure

In this section, we propose an estimation procedure for large integrated coefficients. We first fix some notations. For any given  $p_1$  by  $p_2$  matrix  $\mathbf{U} = (U_{ij})_{i=1,\dots,p_1,j=1,\dots,p_2}$ , let

$$\|\mathbf{U}\|_{\max} = \max_{i,j} |U_{ij}|, \quad \|\mathbf{U}\|_1 = \max_{1 \leq j \leq p_2} \sum_{i=1}^{p_1} |U_{ij}|, \quad \text{and} \quad \|\mathbf{U}\|_{\infty} = \max_{1 \leq i \leq p_1} \sum_{j=1}^{p_2} |U_{ij}|.$$

We denote the Frobenius norm of  $\mathbf{U}$  by  $\|\mathbf{U}\|_F = \sqrt{\text{tr}(\mathbf{U}^\top \mathbf{U})}$ . The matrix spectral norm  $\|\mathbf{U}\|_2$  is the square root of the largest eigenvalue of  $\mathbf{U}\mathbf{U}^\top$ .  $C$ 's denote generic constants whose values are free of  $n$  and  $p$  and may change from appearance to appearance.

From the model (2.1), the instantaneous coefficient  $\beta_t$  satisfies the following equation:

$$\frac{d}{dt}[Y, \mathbf{X}]_t = \beta_t^\top \frac{d}{dt}[\mathbf{X}, \mathbf{X}]_t \text{ a.s.,}$$

where  $[\cdot, \cdot]$  denotes the quadratic variation. The coefficient process  $\beta_t$  is a function of instantaneous volatilities of  $\mathbf{X}$  and  $Y$  as follows:

$$\beta_t = \Sigma_t^{-1} \Sigma_{XY,t} \text{ a.s.,} \quad (3.1)$$

where  $\Sigma_t = \sigma_t \sigma_t^\top$  and  $\Sigma_{XY,t} = \frac{d}{dt}[\mathbf{X}, Y]_t$ . Thus, the instantaneous coefficient can be estimated by the instantaneous volatility estimators. For the finite dimensional case, the instantaneous volatility-based estimation procedure works well (Aït-Sahalia et al., 2020). However, this approach cannot explain the sparse structure (2.4). Furthermore, when the dimensionality of the covariate  $\mathbf{X}$  is larger than the sample size, this approach fails to consistently estimate the instantaneous coefficient. Therefore, the procedure developed for the finite dimension is neither effective nor efficient. In contrast, the direct application of the high-dimensional regression procedure such as the LASSO (Tibshirani, 1996) and Dantzig selector (Candes and Tao, 2007) cannot consistently estimate the integrated coefficients. Specifically, we can rewrite (2.1) as follows:

$$dY_t = \beta_0^\top d\mathbf{X}_t + (\beta_t - \beta_0)^\top d\mathbf{X}_t + dZ_t, \quad (3.2)$$

where  $\beta_0$  is a constant vector. Due to the time-variation of the coefficient process, we have a non-negligible dependent structure between  $\beta_0^\top d\mathbf{X}_t$  and  $(\beta_t - \beta_0)^\top d\mathbf{X}_t$ . This produces a

bias for the usual high-dimensional regression methods. To mitigate the dependency and accommodate the sparse structure of the coefficient process in (2.4), we employ the time-localized Dantzig selection method as follows. Let  $\Delta_i^n A = A_{i\Delta_n} - A_{(i-1)\Delta_n}$  for  $1 \leq i \leq 1/\Delta_n$ , where  $\Delta_n = 1/n$  is the distance between adjacent observation time points. Define

$$\begin{aligned} \mathcal{Y}_i &= (\Delta_{i+1}^n Y, \Delta_{i+2}^n Y, \dots, \Delta_{i+k_n}^n Y)^\top, \quad \mathcal{X}_i = (\Delta_{i+1}^n \mathbf{X}, \Delta_{i+2}^n \mathbf{X}, \dots, \Delta_{i+k_n}^n \mathbf{X})^\top, \quad \text{and} \\ \mathcal{Z}_i &= (\Delta_{i+1}^n Z, \Delta_{i+2}^n Z, \dots, \Delta_{i+k_n}^n Z)^\top, \end{aligned}$$

where  $k_n$  is the number of observations in each window to calculate the local regression. Then, we estimate the sparse instantaneous coefficient as follows:

$$\hat{\beta}_{i\Delta_n} = \arg \min \|\beta\|_1 \quad \text{s.t.} \quad \left\| \frac{1}{k_n \Delta_n} \mathcal{X}_i^\top \mathcal{X}_i \beta - \frac{1}{k_n \Delta_n} \mathcal{X}_i^\top \mathcal{Y}_i \right\|_{\max} \leq \lambda_n, \quad (3.3)$$

where  $\lambda_n$  is a tuning parameter which converges to zero. We specify  $\lambda_n$  in Theorem 1. With the appropriate  $\lambda_n$ , we can show that the proposed Dantzig instantaneous coefficient estimator  $\hat{\beta}_{i\Delta_n}$  is a consistent estimator (see Theorem 1). To estimate the integrated coefficient  $I\beta$  with this consistent estimator, we usually consider the sum of the instantaneous coefficient estimators  $\hat{\beta}_{i\Delta_n}$ 's. However, the Dantzig estimator is biased, so their summation cannot enjoy the law of large numbers properties. For example, the error of the sum of the Dantzig instantaneous coefficient estimators is dominated by the bias terms, and so it has the same convergence rate as that of  $\hat{\beta}_{i\Delta_n}$ . To reduce the effect of the bias, we use a debiasing scheme as follows. We first estimate the inverse matrix of the instantaneous volatility matrix  $\Sigma_{i\Delta_n}$  using the constrained  $\ell_1$ -minimization for inverse matrix estimation (CLIME) (Cai et al., 2011). Let  $\hat{\Omega}_{i\Delta_n}$  be the solution of the following optimization problem:

$$\min \|\Omega\|_1 \quad \text{s.t.} \quad \left\| \frac{1}{k_n \Delta_n} \mathcal{X}_i^\top \mathcal{X}_i \Omega - \mathbf{I} \right\|_{\max} \leq \tau_n, \quad (3.4)$$



where  $\tau_n$  is the tuning parameter specified in Theorem 2. With the CLIME estimator, we adjust the Dantzig instantaneous coefficient estimator as follows:

$$\tilde{\beta}_{i\Delta_n} = \hat{\beta}_{i\Delta_n} + \frac{1}{k_n\Delta_n} \hat{\Omega}_{i\Delta_n}^\top \mathcal{X}_i^\top (\mathcal{Y}_i - \mathcal{X}_i \hat{\beta}_{i\Delta_n}). \quad (3.5)$$

Then, the debiased Dantzig instantaneous coefficient estimator satisfies

$$\tilde{\beta}_{i\Delta_n} - \beta_{0,i\Delta_n} = \frac{1}{k_n\Delta_n} \Omega_{0,i\Delta_n} (\mathcal{X}_i^\top \mathcal{Z}_i + \mathcal{A}_i) + R_i \text{ a.s.}, \quad (3.6)$$

where the subscript 0 represents the true parameter values,  $\mathcal{A}_i$  is a martingale difference defined in (C.11) in Appendix C, and  $R_i$  is a negligible remaining error term (see Theorem 3). We note that the debiasing scheme is usually employed to derive asymptotic normality and to conduct the confidence interval construction or hypothesis testing (Javanmard and Montanari, 2018; Van de Geer et al., 2014; Zhang and Zhang, 2014). However, we adopt the debiasing scheme to improve the integrated coefficient estimation. Specifically, the debiasing scheme helps enjoy the law of large numbers property when averaging the instantaneous coefficient estimators. The integrated coefficient estimator is defined by

$$\widehat{I\beta} = \sum_{i=0}^{[1/(k_n\Delta_n)]-1} \tilde{\beta}_{ik_n\Delta_n} k_n\Delta_n.$$

As discussed above, the debiasing scheme helps improve the element-wise convergence rate of the debiased Dantzig integrated coefficient estimator. However, the debiased Dantzig integrated coefficient estimator does not satisfy the sparsity condition (2.4) due to the bias adjustment. To accommodate the sparsity of the integrated coefficient, we apply the thresholding scheme as follows:

$$\widetilde{I\beta}_i = s(\widehat{I\beta}_i) \mathbf{1}(|\widehat{I\beta}_i| \geq h_n) \quad \text{and} \quad \widetilde{I\beta} = \left(\widetilde{I\beta}_i\right)_{i=1,\dots,p},$$

where  $\mathbf{1}(\cdot)$  is an indicator function, the thresholding function  $s(\cdot)$  satisfies that  $|s(x) - x| \leq h_n$ , and  $h_n$  is a thresholding level specified in Theorem 4. Examples of the thresholding function  $s(x)$  include the hard thresholding function  $s(x) = x$  and the soft thresholding function  $s(x) = x - \text{sign}(x)h_n$ . For the empirical study, we employed the hard thresholding function. We call this the Thresholded dEbiased Dantzig (TED) estimator. We summarize the TED estimation procedure in Algorithm 1, and additional implementation details including a graphical illustration and computational complexity analyses are provided in Appendix A.

**Remark 1.** The time-localized Dantzig method in (3.3) estimates the instantaneous coefficient process by utilizing the relationship (3.1). This intuitive connection allows the method to be naturally extended to accommodate various stylized features of high-frequency financial data, such as microstructure noise and heavy-tailed distributions. The only requirement is that the estimates of instantaneous covariance matrices in the constraint of (3.3) satisfy certain convergence rates, which are discussed in Appendix B. Indeed, several existing studies have addressed these features in the context of volatility estimation (Aït-Sahalia and Xiu, 2017; Barndorff-Nielsen et al., 2011; Fan and Kim, 2018; Kim et al., 2018; Shin and Kim, 2023; Zhang, 2011). Therefore, our approach can be extended by adopting similar ideas. Alternatively, the LASSO method employs a penalized least squares approach to address high-dimensional regression. Under locally constant or mildly time-varying coefficients within each time-localized window, the LASSO method can serve as an alternative to the Dantzig selector (Bickel et al., 2009). Nevertheless, because of its penalized least squares formulation, the LASSO method does not naturally extend to accommodate these features, in contrast to the Dantzig approach. In this sense, the proposed method offers greater flexibility.

---

**Algorithm 1** TED estimation procedure.

---

**Step 1** Estimate the instantaneous coefficient:

$$\widehat{\beta}_{i\Delta_n} = \arg \min \|\beta\|_1 \quad \text{s.t.} \quad \left\| \frac{1}{k_n\Delta_n} \mathcal{X}_i^\top \mathcal{X}_i \beta - \frac{1}{k_n\Delta_n} \mathcal{X}_i^\top \mathcal{Y}_i \right\|_{\max} \leq \lambda_n,$$

where  $\lambda_n = C_\lambda s_p \sqrt{\log p} \left( \sqrt{k_n\Delta_n} + k_n^{-1/2} \right)$  and  $k_n = c_k n^{1/2}$  for some large constants  $C_\lambda$  and  $c_k$ .

**Step 2** Debias the Dantzig instantaneous coefficient estimator:

$$\widetilde{\beta}_{i\Delta_n} = \widehat{\beta}_{i\Delta_n} + \frac{1}{k_n\Delta_n} \widehat{\Omega}_{i\Delta_n}^\top \mathcal{X}_i^\top (\mathcal{Y}_i - \mathcal{X}_i \widehat{\beta}_{i\Delta_n}),$$

where

$$\widehat{\Omega}_{i\Delta_n} = \arg \min \|\Omega\|_1 \quad \text{s.t.} \quad \left\| \frac{1}{k_n\Delta_n} \mathcal{X}_i^\top \mathcal{X}_i \Omega - \mathbf{I} \right\|_{\max} \leq \tau_n,$$

with  $\tau_n = C_\tau \sqrt{\log p} \left( \sqrt{k_n\Delta_n} + k_n^{-1/2} \right)$  for some large constant  $C_\tau$ .

**Step 3** Estimate the integrated coefficient:

$$\widehat{I\beta} = \sum_{i=0}^{\lfloor 1/(k_n\Delta_n) \rfloor - 1} \widetilde{\beta}_{ik_n\Delta_n} k_n\Delta_n.$$

**Step 4** Threshold the debiased Dantzig integrated coefficient estimator:

$$\widetilde{I\beta}_i = s(\widehat{I\beta}_i) \mathbf{1} \left( |\widehat{I\beta}_i| \geq h_n \right) \quad \text{and} \quad \widetilde{I\beta} = \left( \widetilde{I\beta}_i \right)_{i=1, \dots, p},$$

where  $\mathbf{1}(\cdot)$  is an indicator function, the thresholding function  $s(\cdot)$  satisfies that  $|s(x) - x| \leq h_n$ ,  $h_n = C_h b_n$  for some constant  $C_h$ , and  $b_n$  is defined in Theorem 3.

---

## 3.2 Asymptotic results

In this section, we establish the asymptotic properties for the proposed TED estimation procedure. To investigate the asymptotic properties, we need the following technical conditions.

**Assumption 1.**

(a) The volatility process  $\Sigma_t = (\Sigma_{ijt})_{i,j=1, \dots, p}$  satisfies the following Hölder condition:

$$|\Sigma_{ijt} - \Sigma_{ijs}| \leq C |t - s|^{1/2} \quad \text{a.s.}$$

(b)  $\boldsymbol{\mu}_t$ ,  $\boldsymbol{\mu}_{\beta,t}$ ,  $\boldsymbol{\beta}_t$ ,  $\boldsymbol{\nu}_t$ ,  $\boldsymbol{\Sigma}_t$ , and  $\boldsymbol{\Sigma}_{\beta,t} = \boldsymbol{\nu}_{\beta,t} \boldsymbol{\nu}_{\beta,t}^\top$  are a.s. bounded, and  $\|\boldsymbol{\Sigma}_t^{-1}\|_1 \leq C$  a.s.

(c) The drift process  $\boldsymbol{\mu}_{\beta,t} = (\mu_{\beta,1t}, \dots, \mu_{\beta,pt})^\top$  and the volatility process  $\boldsymbol{\Sigma}_{\beta,t} = (\Sigma_{\beta,ijt})_{i,j=1,\dots,p}$  satisfy the following sparsity condition for  $\delta \in [0, 1)$ :

$$\sup_{0 \leq t \leq 1} \sum_{i=1}^p |\mu_{\beta,it}|^\delta \leq s_p \quad \text{and} \quad \sup_{0 \leq t \leq 1} \sum_{i=1}^p |\Sigma_{\beta,iit}|^{\delta/2} \leq s_p \quad \text{a.s.}$$

(d)  $n^{c_1} \leq p \leq c_2 \exp(n^{c_3})$  for some positive constants  $c_1$ ,  $c_2$ , and  $c_3 < 1/8$ , and  $\log p(s_p^2 + \log p + s_{\omega,p}^{2/(1-q)})k_n^{-1} \rightarrow 0$  as  $n, p \rightarrow \infty$ .

(e) The inverse matrix of the volatility matrix process,  $\boldsymbol{\Sigma}_t^{-1} = \boldsymbol{\Omega}_t = (\omega_{ijt})_{i,j=1,\dots,p}$ , satisfies the following sparsity condition:

$$\sup_{0 \leq t \leq 1} \max_{1 \leq i \leq p} \sum_{j=1}^p |\omega_{ijt}|^q \leq s_{\omega,p} \quad \text{a.s.},$$

where  $q \in [0, 1)$  and  $s_{\omega,p}$  is diverging slowly with respect to  $p$ , for example,  $\log p$ .

**Remark 2.** To investigate estimators of time-varying processes, we need continuity conditions such as Assumption 1(a) and the diffusion process structures for  $\mathbf{X}_t$ ,  $Y_t$  and  $\boldsymbol{\beta}_t$  in Section 2. Even if Assumption 1(a) is replaced by the condition that  $\boldsymbol{\Sigma}_t$  has a continuous Itô diffusion process structure with bounded drift and instantaneous volatility processes, we can obtain the same theoretical results with up to  $\sqrt{\log p}$  order. For simplicity, we put Assumption 1(a). The boundedness condition Assumption 1(b) provides sub-Gaussian tails which are often required to investigate high-dimensional inferences. On the other hand, when we investigate the asymptotic behaviors of volatility estimators such as their convergence rate, the boundedness condition can be relaxed to the locally boundedness condition (see Aït-Sahalia and Xiu (2017)). Specifically, Jacod and Protter (2011) showed in Lemma 4.4.9 that if the asymptotic result, such as stable convergence in law or convergence in probability, is satisfied under the boundedness condition, it is also satisfied under the locally bound-

edness condition. Thus, the asymptotic results established in this paper also hold for the locally boundedness condition. The sparsity condition for the coefficient process, Assumption 1(c), is the technical condition for investigating the discretization error of the Dantzig instantaneous coefficient estimator  $\widehat{\beta}_{i\Delta_n}$ . Assumption 1(d) ensures a sufficient number of observations in each time-localized window to estimate and remove the bias at the required convergence rate. Finally, to investigate asymptotic properties of the CLIME estimator, we need the sparse inverse matrix condition Assumption 1(e) (Cai et al., 2011). Similar to (2.4), this condition utilizes the  $\ell_q$ -ball to define a general sparsity class that includes the exact sparsity as a special case. Furthermore, if the smallest eigenvalue of  $\Sigma_t$  is strictly bigger than zero, the Frobenius norm of  $\Omega_t$  is bounded by  $C\sqrt{p}$ . This implies that the inverse matrix,  $\Omega_t$ , cannot be dense with many non-negligible elements; otherwise, the smallest eigenvalue of  $\Sigma_t$  would approach zero, which indicates perfect multicollinearity among the covariates. Since the strict positiveness of the smallest eigenvalue is the minimum requirement to investigate the regression-based models, Assumption 1(e) is reasonable.

In Theorems 1 and 2 below, we establish asymptotic properties for the sparse instantaneous coefficient and inverse matrix. Note that we use subscript 0 for the true parameters.

**Theorem 1.** *Under Assumption 1(a)–(d), let  $k_n = c_k n^c$  for some constants  $c_k$  and  $c \in (1/4, 1/2]$ . For any given positive constant  $a$ , choose  $\lambda_n = C_{\lambda,a} s_p \sqrt{\log p} \left( \sqrt{k_n \Delta_n} + k_n^{-1/2} \right)$  for some large constant  $C_{\lambda,a}$ . Then, we have, for large  $n$ ,*

$$\max_i \|\widehat{\beta}_{i\Delta_n} - \beta_{0,i\Delta_n}\|_{\max} \leq C\lambda_n \quad \text{and} \quad \max_i \|\widehat{\beta}_{i\Delta_n} - \beta_{0,i\Delta_n}\|_1 \leq C s_p \lambda_n^{1-\delta}, \quad (3.7)$$

*with probability greater than  $1 - p^{-a}$ .*

**Theorem 2.** *Under Assumption 1, let  $k_n = c_k n^c$  for some constants  $c_k$  and  $c \in (1/4, 1/2]$ . For any given positive constant  $a$ , choose  $\tau_n = C_{\tau,a} \sqrt{\log p} \left( \sqrt{k_n \Delta_n} + k_n^{-1/2} \right)$  for some large*

constant  $C_{\tau,a}$ . Then, we have, for large  $n$ ,

$$\max_i \|\hat{\mathbf{\Omega}}_{i\Delta_n} - \mathbf{\Omega}_{0,i\Delta_n}\|_{\max} \leq C\tau_n \quad \text{and} \quad \max_i \|\hat{\mathbf{\Omega}}_{i\Delta_n} - \mathbf{\Omega}_{0,i\Delta_n}\|_1 \leq Cs_{\omega,p}\tau_n^{1-q}, \quad (3.8)$$

with probability greater than  $1 - p^{-a}$ .

**Remark 3.** Theorems 1 and 2 show that by choosing  $c = 1/2$ , the estimators for the instantaneous coefficient and inverse matrix have element-wise convergence rates of  $n^{-1/4}$  and  $\ell_1$  convergence rates  $n^{-(1-\delta)/4}$  and  $n^{-(1-q)/4}$ , respectively, with the log order term and the sparsity level term. We note that when choosing the sub-interval length  $k_n = c_k n^{1/2}$  to estimate the instantaneous processes, we have the same order convergence rates of the statistical estimation and time-varying instantaneous process approximation errors. That is, the order  $n^{-1/4}$  is optimal for estimating each element of the instantaneous process; thus, the convergence rates are optimal up to log order.

The Dantzig instantaneous coefficient estimator has a near-optimal convergence rate as shown in Theorem 1. However, as discussed in the previous section, it is a biased estimator, which causes some non-negligible estimation errors when estimating the integrated coefficient. To tackle this problem, we employ debiasing schemes with the consistent CLIME estimator as in (3.5), and in the following theorem, we investigate its asymptotic benefits.

**Theorem 3.** Under the assumptions in Theorems 1–2, we choose  $k_n = c_k n^{1/2}$  for some constant  $c_k$ . Then, we have for all  $i$ ,

$$\tilde{\beta}_{i\Delta_n} - \beta_{0,i\Delta_n} = \frac{1}{k_n \Delta_n} \mathbf{\Omega}_{0,i\Delta_n} (\mathcal{X}_i^\top \mathcal{Z}_i + \mathcal{A}_i) + R_i, \quad (3.9)$$

where  $\mathcal{A}_i$  is defined in (C.11) and

$$\max_i \|R_i\|_{\max} \leq C \left\{ s_p^{2-\delta} (\log p / n^{1/2})^{(2-\delta)/2} + s_p s_{\omega,p} (\log p / n^{1/2})^{(2-q)/2} + s_p (\log p)^{3/2} / n^{1/2} \right\}, \quad (3.10)$$

with probability greater than  $1 - p^{-a}$  for any given positive constant  $a$ . Furthermore, we have, with probability greater than  $1 - p^{-a}$  for any given positive constant  $a$ ,

$$\|\widehat{I\beta} - I\beta_0\|_{\max} \leq Cb_n, \quad (3.11)$$

where  $b_n = s_p^{2-\delta}(\log p/n^{1/2})^{(2-\delta)/2} + s_p s_{\omega,p}(\log p/n^{1/2})^{(2-q)/2} + s_p(\log p)^{3/2}/n^{1/2}$ .

**Remark 4.** The debiased Dantzig instantaneous coefficient is decomposed by the martingale difference term  $\mathcal{X}_i^\top \mathcal{Z}_i + \mathcal{A}_i$  and the non-martingale remaining term  $R_i$ . The martingale difference term can enjoy the law of large numbers property, so the integrated coefficient estimator has a faster convergence rate than the Dantzig instantaneous coefficient estimator. The remaining non-martingale terms have the same order as those of the martingale terms for the integrated coefficient estimator. Unlike the biased Dantzig estimator, the non-martingale remaining terms do not impact on the integrated coefficient estimator.

**Remark 5.** Theorem 3 shows the element-wise convergence rate for the debiased Dantzig integrated coefficient. When we have the exact sparse coefficient and inverse matrix processes, that is,  $\delta = q = 0$ , the debiased Dantzig integrated coefficient estimator has the convergence rate  $s_p(s_p + s_{\omega,p})(\log p)^{3/2}/n^{1/2}$ . The  $n^{1/2}$  term is related with the sample size, which is known as the optimal rate. The  $(\log p)^{3/2}$  term comes from handling the high-dimensional error bound. Usually, in high-dimensional literature, we have  $\sqrt{\log p}$ , but the debiased Dantzig integrated coefficient estimator has  $(\log p)^{3/2}$  due to the handling of the high-dimensional error bounds for estimating two coefficients, such as the instantaneous coefficient and the integrated coefficient, and bounding the random processes. Finally, the  $s_p$  and  $s_{\omega,p}$  terms represent the sparsity levels for the coefficient and inverse volatility matrix. High-dimensional literature commonly assumes the sparsity level to be negligible; hence, we have the convergence rate  $n^{-1/2}$  with up to  $\log p$  order.

Theorem 3 indicates that, using the debiasing scheme, we obtain well-performing input

integrated coefficient estimator  $\widehat{I\beta}$ . As described in Section 3.1, we then apply the thresholding scheme to  $\widehat{I\beta}$  to account for the sparsity and obtain the TED estimator. In the following theorem, we establish the  $\ell_1$  convergence rate of the TED estimator.

**Theorem 4.** *Under the assumptions in Theorems 1–2, let  $k_n = c_k n^{1/2}$  for some constant  $c_k$ . For any given positive constant  $a$ , choose  $h_n = C_{h,a} b_n$  for some constant  $C_{h,a}$ , where  $b_n$  is defined in Theorem 3. Then, we have, with probability greater than  $1 - p^{-a}$ ,*

$$\|\widetilde{I\beta} - I\beta_0\|_1 \leq C s_p b_n^{1-\delta}. \quad (3.12)$$

Theorem 4 shows that the TED estimator is a consistent estimator in terms of the  $\ell_1$  norm under the sparsity condition (2.4). When estimating the integrated coefficient without the debiasing step, we can obtain the convergence rate  $s_p(s_p \sqrt{\log p n}^{-1/4})^{1-\delta}$ . The benefit of applying the debiasing scheme is the difference between  $b_n$  and  $s_p \sqrt{\log p n}^{-1/4}$ . Under the sparsity condition,  $b_n$  is  $n^{-\{2-(\delta \vee q)\}/4}$  with  $\log p$  order for  $\delta, q \in [0, 1]$ , which is faster than the convergence rate of the Dantzig integrated coefficient estimator. Therefore, the TED estimator has the faster convergence rate.

### 3.3 Extension to jump diffusion processes

In financial practice, we often observe jumps. To reflect this, we can extend the continuous diffusion process (2.1) to the jump diffusion process as follows:

$$dY_t = dY_t^c + dY_t^J, \quad dY_t^c = \beta_t^\top d\mathbf{X}_t^c + dZ_t, \quad \text{and} \quad dY_t^J = J_t^y d\Lambda_t^y, \quad (3.13)$$

where  $Y_t^c$  and  $\mathbf{X}_t^c$  are the continuous part of  $Y_t$  and  $\mathbf{X}_t$ , respectively,  $J_t^y$  is the jump size, and  $\Lambda_t^y$  is the Poisson process with the bounded intensity. The covariate process  $\mathbf{X}_t$  is

$$d\mathbf{X}_t = d\mathbf{X}_t^c + d\mathbf{X}_t^J, \quad d\mathbf{X}_t^c = \boldsymbol{\mu}_t dt + \boldsymbol{\sigma}_t d\mathbf{B}_t, \quad \text{and} \quad d\mathbf{X}_t^J = \mathbf{J}_t d\Lambda_t, \quad (3.14)$$



where  $\mathbf{J}_t = (J_{1t}, \dots, J_{pt})^\top$  is a jump size process and  $\mathbf{\Lambda}_t = (\Lambda_{1t}, \dots, \Lambda_{pt})^\top$  is a  $p$ -dimensional Poisson process with bounded intensities. We assume that the Poisson processes  $\Lambda_t^y$  and  $\mathbf{\Lambda}_t$  are independent of  $\boldsymbol{\sigma}_t$  and  $\boldsymbol{\beta}_t$ . Under this jump diffusion model, we can still use the proposed estimation procedure, but we cannot observe the continuous diffusion process. To tackle this problem, we first detect the jumps from the observed stock log-return data. For example, we use the truncation method as follows. Define

$$\widehat{\mathcal{Y}}_i^c = \left( \Delta_{i+1}^n \widehat{Y}^{c\top}, \Delta_{i+2}^n \widehat{Y}^{c\top}, \dots, \Delta_{i+k_n}^n \widehat{Y}^{c\top} \right)^\top \text{ and } \widehat{\mathcal{X}}_i^c = \left( \Delta_{i+1}^n \widehat{\mathbf{X}}^c, \Delta_{i+2}^n \widehat{\mathbf{X}}^c, \dots, \Delta_{i+k_n}^n \widehat{\mathbf{X}}^c \right)^\top \quad (3.15)$$

where  $\mathbf{1}_{\{\cdot\}}$  is an indicator function,  $k_n$  is the number of observations in each window used to calculate the local regression,

$$\Delta_i^n \widehat{Y}^c = \Delta_i^n Y \mathbf{1}_{\{|\Delta_i^n Y| \leq u_n\}}, \quad \Delta_i^n \widehat{\mathbf{X}}^c = \left( \Delta_i^n X_j \mathbf{1}_{\{|\Delta_i^n X_j| \leq v_{j,n}\}} \right)_{j=1, \dots, p},$$

and  $u_n$  and  $v_{j,n}$ ,  $j = 1, \dots, p$ , are the truncation levels. We employ  $u_n = C_u s_p \sqrt{\log pn}^{-\varrho}$  and  $v_{j,n} = C_{j,v} \sqrt{\log pn}^{-\varrho}$  for  $\varrho \in [15/32, 1/2)$  and some constants  $C_u$  and  $C_{j,v}$ ,  $j = 1, \dots, p$ . In the numerical study, we adopt the usual choice in the literature (Aït-Sahalia et al., 2020; Aït-Sahalia and Xiu, 2019b). That is, we use

$$u_n = 3n^{-0.47} \sqrt{BV^Y} \quad \text{and} \quad v_{j,n} = 3n^{-0.47} \sqrt{BV_j}, \quad (3.16)$$

where the bipower variations  $BV^Y = \frac{\pi}{2} \sum_{i=2}^n |\Delta_{i-1}^n Y| \cdot |\Delta_i^n Y|$  and  $BV_j = \frac{\pi}{2} \sum_{i=2}^n |\Delta_{i-1}^n X_j| \cdot |\Delta_i^n X_j|$ . Then, to estimate the integrated coefficient  $I\beta$ , we employ the estimation method in Section 3.1 using  $\widehat{\mathcal{Y}}_i^c$  and  $\widehat{\mathcal{X}}_i^c$  instead of  $\mathcal{Y}_i$  and  $\mathcal{X}_i$ . We denote the jump-adjusted TED estimator by  $\widetilde{I\beta}^c$ . In the following theorem, we investigate the asymptotic property of the jump-adjusted TED estimator.

**Theorem 5.** *Under the models (3.13)–(3.14), let assumptions in Theorem 4 hold. Then, we*

have, with probability greater than  $1 - p^{-a}$  for any given positive constant  $a$ ,

$$\|\widetilde{I\beta}^c - I\beta_0\|_1 \leq C s_p b_n^{1-\delta}. \quad (3.17)$$

Theorem 5 shows that the jump-adjusted TED estimator has the same convergence rate obtained in Theorem 4. Therefore, we conclude that the jumps can be detected well and that their effects can be mitigated.

### 3.4 Discussion on the tuning parameter selection

To implement the TED estimation procedure, we need to choose the tuning parameters. In this section, we discuss how to select the tuning parameters for the numerical studies. We first obtain  $\Delta_i^n \widehat{Y}^c$  and  $\Delta_i^n \widehat{\mathbf{X}}^c$  with the truncation levels defined in (3.16). Then, to handle the scale issue, we standardize each column of  $\widehat{\mathbf{Y}}_i^c$  and  $\widehat{\mathbf{X}}_i^c$  to have a mean of 0 and a variance of 1. The re-scaling is conducted after obtaining the TED estimator. For the local regression stage (3.3), we choose  $k_n = \lceil n^{1/2} \rceil$ . Also, we select

$$\lambda_n = c_\lambda n^{-1/4} (\log p)^{3/2}, \quad \tau_n = c_\tau n^{-1/4} \sqrt{\log p}, \quad \text{and} \quad h_n = c_h n^{-1/2} (\log p)^{3/2}, \quad (3.18)$$

where  $c_\lambda$ ,  $c_\tau$ , and  $c_h$  are tuning parameters. In the simulation and empirical studies, we choose  $c_\lambda \in [0.1, 10]$  that minimizes the 5-fold cross-validation (CV) error, defined as the average squared prediction error on the validation sets. Also, we select  $c_\tau \in [0.1, 10]$  by minimizing the following loss function:

$$\text{tr} \left[ \left( \frac{1}{k_n \Delta_n} \widehat{\mathbf{X}}_i^{c\top} \widehat{\mathbf{X}}_i^c \widehat{\boldsymbol{\Omega}}_{i\Delta_n} - \mathbf{I}_p \right)^2 \right],$$

where  $\mathbf{I}_p$  is the  $p$ -dimensional identity matrix. Finally, we choose  $c_h$  using a leave-one-out cross-validation scheme as follows. We define the  $j$ th leave-one-block-out integrated

coefficient as follows:

$$\widehat{I\beta}_{(-j)} = \sum_{i=0, i \neq j}^{[1/(k_n \Delta_n)]-1} \widetilde{\beta}_{ik_n \Delta_n} \frac{k_n \Delta_n}{1 - k_n \Delta_n}.$$

We then define the TED estimator with the tuning parameter  $c_h$  and  $\widehat{I\beta}_{(-j)}$  as follows:

$$\widetilde{I\beta}_{(-j)}(c_h) = s(\widehat{I\beta}_{(-j)}) \mathbf{1}(|\widehat{I\beta}_{(-j)}| \geq h_n),$$

where  $h_n = c_h n^{-1/2} (\log p)^{3/2}$ . We then select  $c_h \in [0.01, 10]$  that minimizes the following loss function:

$$k_n \Delta_n \sum_{j=0}^{[1/(k_n \Delta_n)]-1} \left( \mathcal{Y}_j - \widehat{\mathcal{X}}_j^c \widetilde{I\beta}_{(-j)}(c_h) \right)^\top \left( \mathcal{Y}_j - \widehat{\mathcal{X}}_j^c \widetilde{I\beta}_{(-j)}(c_h) \right).$$

## 4 A simulation study

In this section, we conducted simulations to check the finite sample performance of the proposed TED estimator. We generated data from the time series regression jump diffusion model (3.13)–(3.14). We considered two types of coefficient processes, time-varying and constant coefficients. Detailed descriptions of the simulation setup are provided in Appendix D. We set  $p = 100$  with  $s_p = \lceil \log p \rceil = 4$  effective covariates, and varied sample sizes  $n = 1000, 2000, 4000$ . We repeated the simulation 200 times.

To implement the TED estimation procedure, we used the hard thresholding function  $s(x) = x$  and employed the tuning parameter selection method discussed in Section 3.4. To illustrate how effectively the TED estimator captures the time-varying behaviors, Appendix E provides trajectory plots of the true coefficients along with the debiased instantaneous coefficient estimates. The results in Appendix E illustrate that the TED estimator effectively captures the temporal dynamics of the true coefficients.

For the purposes of comparison, we considered the integrated coefficient estimator proposed by Aït-Sahalia et al. (2020). We note that, for small  $p$ , one can account for the time

variation of the coefficient process. We call this the AKX estimator. Specifically, the AKX estimator is calculated as follows:

$$\widehat{\boldsymbol{\beta}}_{i\Delta_n}^{\text{AKX}} = (\widehat{\mathcal{X}}_i^{c\top} \widehat{\mathcal{X}}_i^c)^{-1} \widehat{\mathcal{X}}_i^{c\top} \widehat{\mathcal{Y}}_i^c \quad \text{and} \quad \widetilde{I\boldsymbol{\beta}}^{\text{AKX}} = \sum_{i=0}^{[1/(K_n\Delta_n)]-1} \widehat{\boldsymbol{\beta}}_{iK_n\Delta_n}^{\text{AKX}} K_n\Delta_n, \quad (4.1)$$

where  $\widehat{\mathcal{X}}_i^c$  and  $\widehat{\mathcal{Y}}_i^c$  are defined in (3.15) and we used  $K_n = [n^{0.47}]$  instead of  $k_n = [n^{0.5}]$ . For  $\widehat{\mathcal{X}}_i^{c\top} \widehat{\mathcal{X}}_i^c$  in (4.1), we added  $10^{-4}\mathbf{I}_p$  to avoid the singularity coming from the ultra high-dimensionality. We also employed regression estimators that can handle the sparsity of the high-dimensional coefficient process (without accounting for time-varying coefficients), such as LASSO (LAS), Ridge (RID), elastic net (ELA), SCAD (SCA), Bayesian LASSO (BAY), Dantzig (DAN), and their adaptive versions, such as adaptive LASSO (ALAS), adaptive Ridge (ARID), adaptive elastic net (AELA), adaptive SCAD (ASCA), and adaptive Dantzig (ADAN), as benchmarks (Candes and Tao, 2007; Fan and Li, 2001; Park and Casella, 2008; Tibshirani, 1996; Zou, 2006; Zou and Hastie, 2005; Zou and Zhang, 2009). The tuning parameters for these benchmark estimators were selected to minimize the 5-fold CV errors, consistent with the approach used for the TED estimator. We calculated the average estimation errors under the max norm,  $\ell_1$  norm, and  $\ell_2$  norm.

Figure 1 plots the log max,  $\ell_1$ , and  $\ell_2$  norm errors of TED and benchmarks for the time-varying and constant coefficient processes with  $p = 100$  and  $n = 1000, 2000, 4000$ . From Figure 1, we find that the estimation errors of the TED estimator are decreasing as the number of high-frequency observations increases. For the time-varying coefficient process, the TED estimator outperforms other estimators. This may be because the proposed TED estimation method can account for both time variation and the high-dimensionality of the coefficient process, while the other benchmark estimators fail to explain one of them. For the constant coefficient process, TED and ALAS, ADAN, and AELA show better performance than the other benchmark estimators. This is probably due to the fact that the other estimators cannot adequately handle the curse of dimensionality or the bias caused by penalties

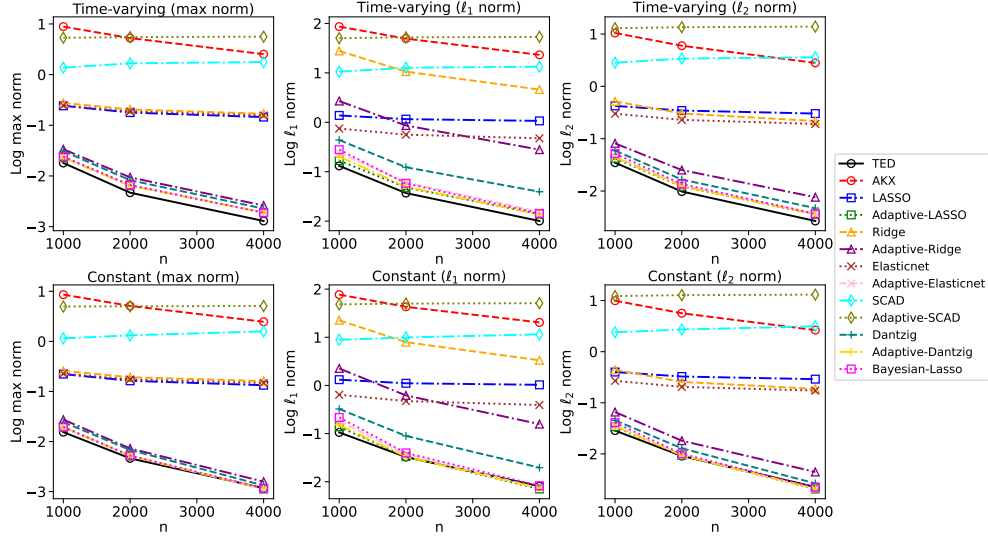


Figure 1: The log max,  $\ell_1$ , and  $\ell_2$  norm error plots of TED and benchmarks for  $p = 100$  and  $n = 1000, 2000, 4000$ .

imposed to induce sparsity.

Finally, we evaluated the variable selection accuracy of the TED estimator and benchmark methods using precision and recall metrics. Table 1 presents the average precision and recall across different sample sizes and benchmarks for the time-varying and constant coefficient processes with  $n = 1000, 2000, 4000$ . From Table 1, for the time-varying coefficient process, we observe that while several methods achieve perfect precision or recall separately, only TED and ELA simultaneously maintain both precision and recall above 0.95 for  $n = 4000$ . When comparing TED with ELA, TED shows higher recall. This indicates that TED is more effective in correctly identifying all significant factors. In the case of the constant coefficient process, TED achieves reasonably high precision and recall, 0.982 and 1, respectively, while LAS and ELA achieve perfect precision and recall. This may be because, under the constant coefficient process, TED cannot significantly benefit from its complex estimation procedure, which is primarily designed to handle time-varying coefficients. These results suggest that the TED estimator effectively accounts for the time variation and high-dimensionality of the coefficient process and is robust to the coefficient process structure.

Table 1: Average precision and recall of variable selection for TED and benchmarks across different sample sizes  $n$ .

<b>Time-varying</b>													
<i>Precision</i>													
$n$	TED	AKX	LAS	ALAS	RID	ARID	ELA	AELA	SCA	ASCA	DAN	ADAN	BAY
1000	0.927	0.040	1.000	0.802	0.040	0.040	0.996	0.639	1.000	1.000	0.323	0.721	0.684
2000	0.967	0.040	1.000	0.888	0.040	0.040	1.000	0.769	1.000	1.000	0.308	0.830	0.836
4000	0.971	0.040	1.000	0.939	0.040	0.040	1.000	0.862	1.000	1.000	0.289	0.912	0.925
<i>Recall</i>													
$n$	TED	AKX	LAS	ALAS	RID	ARID	ELA	AELA	SCA	ASCA	DAN	ADAN	BAY
1000	0.995	1.000	0.930	0.995	1.000	1.000	0.990	0.995	0.750	0.263	0.998	0.995	0.994
2000	0.996	1.000	0.924	0.994	1.000	1.000	0.988	0.995	0.705	0.254	0.999	0.995	0.996
4000	0.996	1.000	0.926	0.995	1.000	1.000	0.990	0.996	0.680	0.251	0.999	0.995	0.998
<b>Constant</b>													
<i>Precision</i>													
$n$	TED	AKX	LAS	ALAS	RID	ARID	ELA	AELA	SCA	ASCA	DAN	ADAN	BAY
1000	0.926	0.040	1.000	0.805	0.040	0.040	0.999	0.706	1.000	1.000	0.337	0.772	0.714
2000	0.962	0.040	1.000	0.911	0.040	0.040	1.000	0.813	1.000	1.000	0.324	0.901	0.870
4000	0.982	0.040	1.000	0.978	0.040	0.040	1.000	0.937	1.000	1.000	0.320	0.960	0.939
<i>Recall</i>													
$n$	TED	AKX	LAS	ALAS	RID	ARID	ELA	AELA	SCA	ASCA	DAN	ADAN	BAY
1000	1.000	1.000	0.996	1.000	1.000	1.000	1.000	1.000	0.904	0.251	1.000	1.000	1.000
2000	1.000	1.000	1.000	1.000	1.000	1.000	1.000	1.000	0.895	0.250	1.000	1.000	1.000
4000	1.000	1.000	1.000	1.000	1.000	1.000	1.000	1.000	0.856	0.250	1.000	1.000	1.000

## 5 An empirical study

We applied the proposed TED estimator to real high-frequency trading data from January 2013 to December 2020. We took stock price data from the End of Day website (<https://eoddata.com>) and obtained 5-min log-price data using the previous tick scheme (Wang and Zou, 2010; Zhang, 2011), where half trading days were excluded. We considered the log-prices of the five assets as the dependent processes. Specifically, we selected Apple Inc. (AAPL), Berkshire Hathaway Inc. (BRK.B), General Motors Company (GM), Alphabet Inc. (GOOG), and Exxon Mobil Corporation (XOM). These firms are the top market value stocks in five global industrial classification standards (GICS) sectors: information technology, financials, consumer discretionary, communication services, and energy.

For the covariates, we used the high-frequency factor zoo dataset provided by Aletti (2022), which is publicly available on the author’s website. This dataset contains 272 portfolios: 218 characteristic-sorted factor portfolios, 48 industry portfolios, and the six Fama-French portfolios. Here, the six Fama-French portfolios include market (MKT), value (HML), size (SMB), profitability (RMW), investment (CMA), and momentum (MOM) factors.

To examine the practical advantage of allowing time-varying coefficients, we first conducted a test for coefficient constancy based on the kernel estimation approach of Ang and Kristensen (2012). Since the approach of Ang and Kristensen (2012) cannot handle high-dimensionality, we implemented the test with the six Fama-French factors, which serve as a canonical benchmark in asset pricing (Asness et al., 2013; Barroso and Santa-Clara, 2015; Carhart, 1997; Fama and French, 2015, 2016). For each asset and month, we computed the test statistic in Theorem 3 of Ang and Kristensen (2012) to evaluate the joint null hypothesis that the six Fama-French factor coefficients are constant within the month. Across five assets and 96 months, the total number of tests was 480. The rejection rates at the 5%, 1%, and 0.1% significance levels are 0.996, 0.994, and 0.979, respectively. This result indicates the importance of accommodating time-varying coefficients, which motivates the use of the TED procedure.

The tuning parameters for the TED estimator were selected based on Section 3.4. We additionally conducted an analysis to examine how the choice of tuning parameters affects the TED estimator in Appendix F. The results indicate that the performance of TED is sensitive to the choice of parameters and also highlight the effectiveness of the proposed tuning parameter selection procedure. Since the AKX estimator is designed for the finite dimension, we also employed the AKX6 estimator. The AKX6 estimator employs the same estimation method as the AKX estimator except that it only uses the six Fama-French factors as factor candidates. We also employed OLS with the six factors (OLS6) along with the benchmark estimators used in the simulation study, namely, LAS, ALAS, RID, ARID,

ELA, AELA, SCA, ASCA, BAY, DAN, and ADAN.

Table 2: The annual average in-sample and out-of-sample  $R^2$  for the TED, AKX, AKX6, and various regression estimators across the five assets.

Period	RV (%)	In-sample $R^2$														
		TED	AKX	AKX6	OLS6	LAS	ALAS	RID	ARID	ELA	AELA	SCA	ASCA	BAY	DAN	ADAN
whole	12.0	0.539	0.309	0.066	0.208	0.465	0.591	0.602	0.613	0.512	0.603	0.475	0.257	0.571	0.606	0.610
2013	7.9	0.667	0.322	0.038	0.191	0.554	0.728	0.749	0.753	0.633	0.742	0.562	0.301	0.732	0.745	0.751
2014	8.8	0.525	0.272	0.045	0.184	0.445	0.585	0.597	0.607	0.495	0.599	0.457	0.223	0.556	0.601	0.605
2015	10.2	0.573	0.348	0.072	0.241	0.510	0.624	0.636	0.648	0.547	0.637	0.521	0.331	0.616	0.640	0.645
2016	10.0	0.570	0.324	0.068	0.218	0.494	0.616	0.627	0.635	0.540	0.625	0.506	0.333	0.598	0.628	0.632
2017	5.5	0.453	0.205	0.018	0.143	0.384	0.508	0.520	0.530	0.428	0.522	0.391	0.209	0.494	0.524	0.528
2018	13.0	0.586	0.391	0.112	0.269	0.518	0.625	0.642	0.647	0.556	0.636	0.525	0.292	0.606	0.639	0.644
2019	9.1	0.515	0.288	0.050	0.199	0.441	0.559	0.570	0.581	0.486	0.569	0.452	0.243	0.541	0.574	0.576
2020	22.8	0.425	0.325	0.124	0.220	0.374	0.483	0.479	0.505	0.408	0.492	0.383	0.122	0.428	0.500	0.502
Period	RV (%)	Out-of-sample $R^2$														
		TED	AKX	AKX6	OLS6	LAS	ALAS	RID	ARID	ELA	AELA	SCA	ASCA	BAY	DAN	ADAN
whole	12.0	0.482	0.286	0.060	0.201	0.432	0.459	0.474	0.468	0.460	0.450	0.440	0.246	0.376	0.443	0.414
2013	7.9	0.613	0.308	0.038	0.189	0.520	0.609	0.621	0.618	0.577	0.603	0.525	0.289	0.522	0.600	0.570
2014	8.8	0.475	0.251	0.039	0.176	0.419	0.448	0.468	0.462	0.447	0.437	0.430	0.215	0.369	0.435	0.407
2015	10.2	0.505	0.318	0.063	0.233	0.471	0.494	0.493	0.491	0.492	0.485	0.478	0.309	0.392	0.473	0.443
2016	10.0	0.510	0.306	0.067	0.212	0.461	0.488	0.503	0.498	0.488	0.481	0.468	0.316	0.395	0.479	0.448
2017	5.5	0.398	0.185	0.017	0.137	0.350	0.364	0.386	0.375	0.374	0.349	0.357	0.199	0.289	0.346	0.319
2018	13.0	0.538	0.355	0.088	0.255	0.492	0.517	0.527	0.526	0.513	0.511	0.503	0.290	0.455	0.498	0.479
2019	9.1	0.461	0.271	0.056	0.192	0.407	0.435	0.446	0.444	0.435	0.423	0.416	0.228	0.355	0.425	0.382
2020	22.8	0.366	0.294	0.112	0.212	0.347	0.331	0.356	0.342	0.363	0.322	0.354	0.126	0.244	0.305	0.275

To investigate the performance of the TED estimator and benchmarks, we first calculated the monthly in-sample and out-of-sample  $R^2$  from the monthly integrated coefficient estimates. We obtained the out-of-sample  $R^2$  using the integrated coefficient estimates from the previous month. Then, we calculated the annual average  $R^2$  over the five assets and available months within each year. Table 2 reports the annual average in-sample and out-of-sample  $R^2$  for the TED and benchmarks. RV is the annualized realized volatility of the MKT factor for each period. It is computed as the square root of the sum of squared 5-minute returns and reported in percent. We included RV to examine how the performance of TED varies across different levels of market volatility. From Table 2, we find that the average out-of-sample  $R^2$  of TED exceeds all benchmarks. Furthermore, its annual average out-of-sample  $R^2$  exceeds those of the other benchmarks in every year except 2013, regardless of RV. This is probably because only the TED estimator can account for both the high-dimensionality and time-varying nature of the coefficient process. In terms of in-sample  $R^2$ , TED does not yield the highest value. This is because conventional penalized regression methods aim to maximize



the global penalized in-sample fit, while TED maximizes the penalized in-sample fit within each time-localized window. Since coefficients vary over time, integrated coefficients obtained by aggregating local estimates do not necessarily guarantee the highest in-sample  $R^2$ . Among the regression-based models (without handling time-varying coefficients), RIDGE yields the highest average out-of-sample  $R^2$ . One possible reason for this observation is the presence of time-varying sparsity patterns. If the sparsity patterns vary significantly over time, the support of active covariates aggregated across periods becomes substantially larger, resulting in a denser regime. In this scenario, RID is expected to outperform sparsity-based penalties such as LAS, because the  $\ell_2$  penalty provides more appropriate shrinkage when the aggregated support is enlarged. We also note that TED effectively captures these time-varying sparsity patterns.

To examine the sensitivity of our results to methodological choices—such as tuning parameter selection, alternative approaches for estimating instantaneous coefficients, and an alternative inverse covariance estimation method—we conducted additional analyses. Although our baseline setting generally outperformed alternative choices, other methodological choices provided comparable results. These results confirm the robustness of our main findings. In addition, we compared the predictive accuracy of TED by evaluating the mean absolute error (MAE) of the one-step-ahead fitted returns. We confirmed that TED consistently outperformed other approaches in terms of this MAE as well. We also evaluated the out-of-sample performance at various sampling frequencies (5-, 10-, and 30-min). Details can be found in Appendix F.

Now, we investigate the TED estimation results. Figure 2 shows boxplots of the integrated coefficients for the ten most influential factors, specifically those selected based on the largest average absolute values for each asset. Figure 3 plots the absolute sum of the monthly integrated coefficients from the TED estimation procedure within each of the 15 factor clusters for the five assets across time. The 15 clusters consist of the 13 factor clusters

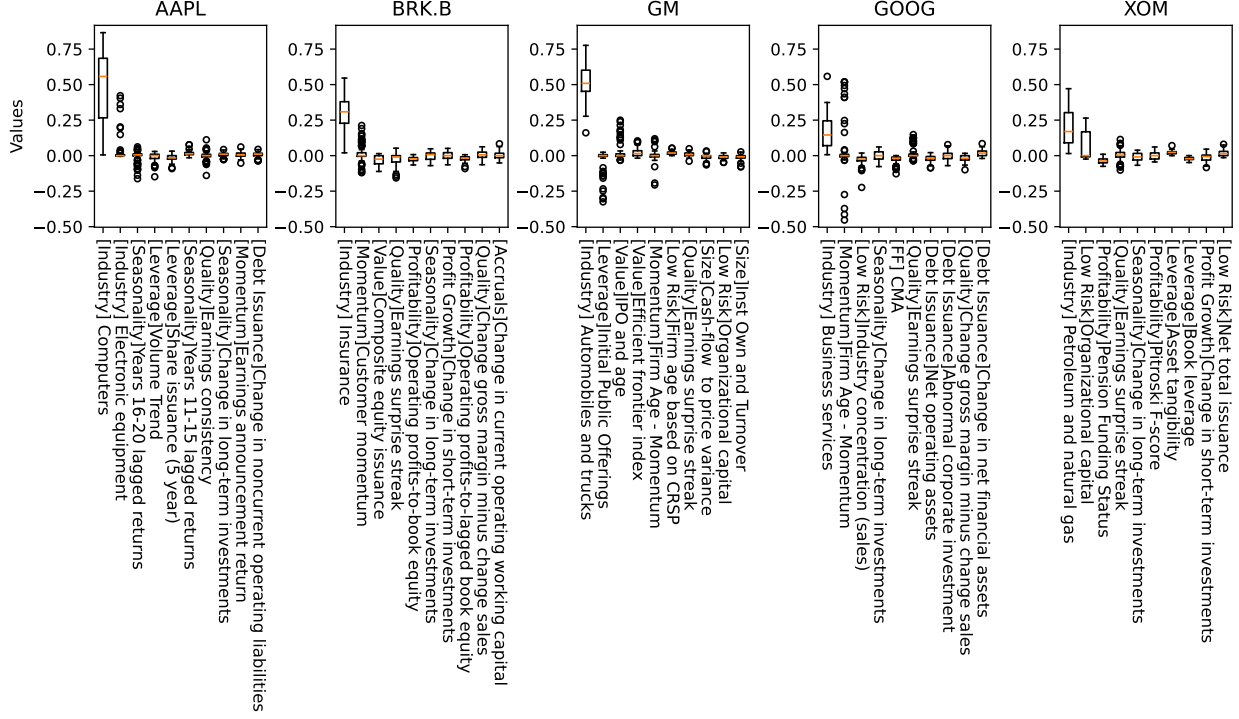


Figure 2: Boxplots of integrated coefficients for the top 10 most influential factors in the factor zoo data.

in Jensen et al. (2023), the FF cluster including the Fama-French five factors and the momentum factor, and the Industry cluster covering the industry factors of Fama and French (1997). From Figures 2–3, we find that the largest coefficient corresponds to the asset’s own industry. This may reflect the strong explanatory power of industry factors compared to other factors. From Figure 3, we also find that the value of the integrated coefficient varies over time and that most of the  $\ell_1$ -norms of the integrated coefficients are less than 3. Since sparsity levels were determined in a data-driven manner via cross-validation, this result may suggest that the sparsity condition (2.4) holds empirically for some  $\delta \in [0, 1)$ .

Several individual factors played a significant role in most periods. Among these, we focus on the three most frequent factors for each of the five assets, and Figure 4 illustrates their integrated coefficients. For example, AAPL has Computers, Electronic equipment, and Seasonality (Years 16-20 lagged returns); BRK.B has Insurance, Customer momentum, and Composite equity issuance; GM has Automobiles and trucks, Initial Public Offerings, and

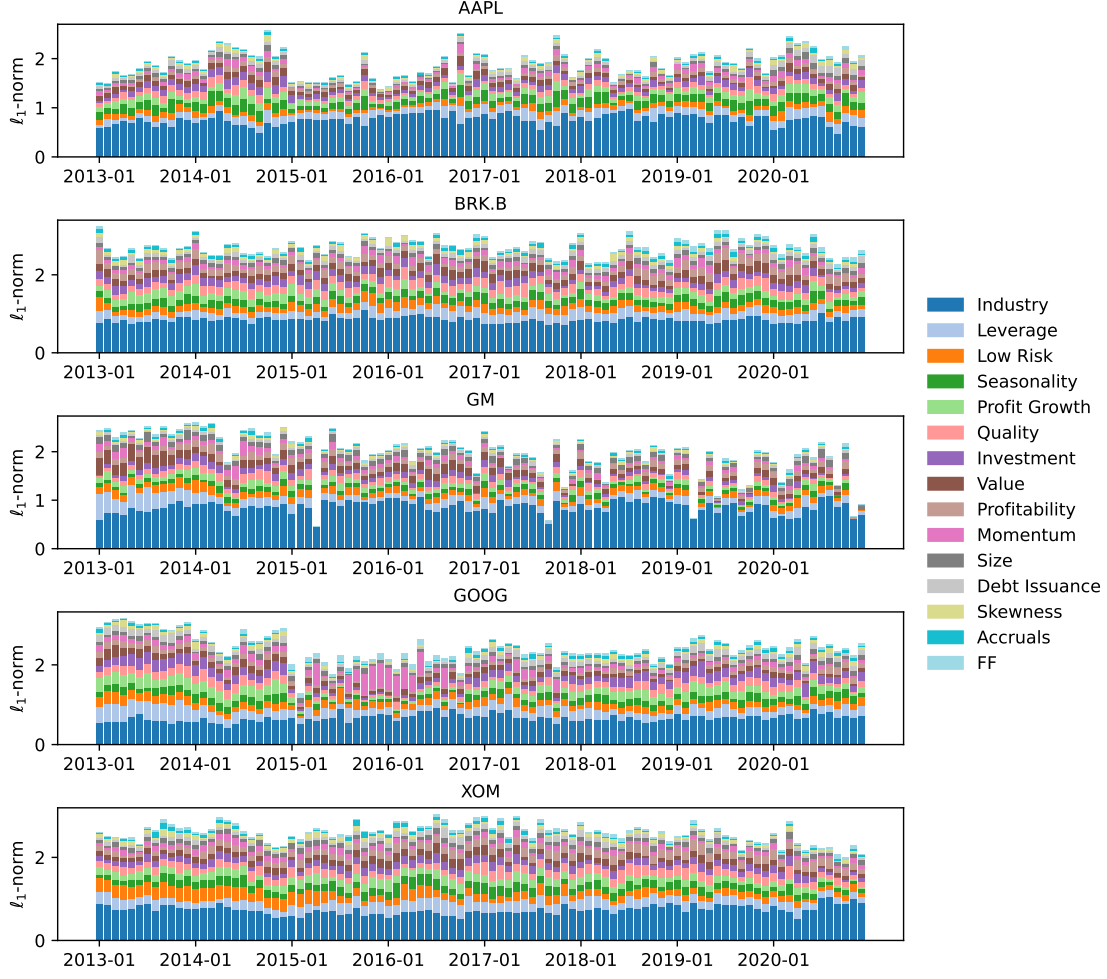


Figure 3: Stacked bar charts of the absolute sum of the monthly integrated coefficients from the TED estimation procedure within each factor cluster for the five assets across 15 factor clusters. The 15 clusters comprise the 13 factor clusters in Jensen et al. (2023), the FF cluster including the Fama-French five factors and the momentum factor, and the Industry cluster covering the industry factors of Fama and French (1997).

IPO and age; GOOG has Business services, Firm Age-Momentum, and Industry concentration (sales); and XOM has Petroleum and natural gas, Organizational capital, and Pension funding status. Among these factors, the industry factors generally exhibit the largest integrated coefficients. Moreover, the coefficient values of the three most frequent factors vary over time, while other factors are significant only for some periods. To illustrate the time-varying nature of factor coefficients more clearly, we examine the specific case of AAPL. Specifically, while the Computers industry factor generally drives AAPL, the Electronic

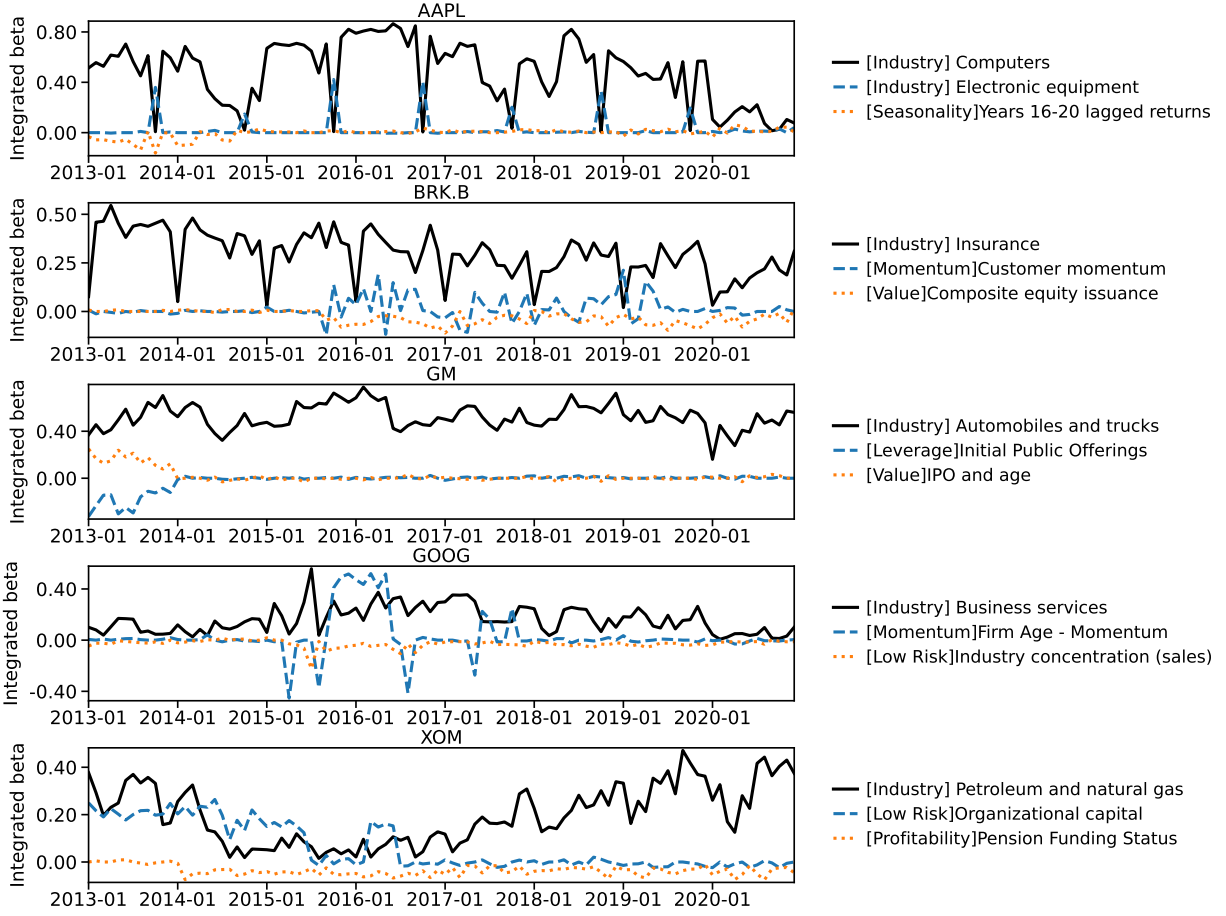


Figure 4: The integrated coefficients from the TED estimation procedure for the three most frequent factors from the factor zoo for each of the five assets.

equipment industry factor consistently emerges as significant around September each year, except for 2020. This pattern likely reflects Apple’s seasonal new product announcements, suggesting that its performance becomes temporarily aligned with electronic components supply chains.

Finally, to interpret the results from the perspective of canonical asset pricing factors, we examined the integrated coefficients of the Fama-French five factors and the momentum factor. The results of this analysis are provided in Appendix F.

From these results, we can infer that the coefficient processes are sparse and time-varying. Hence, incorporating these features is important to account for market dynamics. The proposed TED procedure can provide an effective tool for dealing with these issues when

analyzing market dynamics using high-frequency data.

## 6 Conclusion

In this paper, we proposed a novel Thresholding dEbiased Dantzig (TED) estimation procedure that can accommodate the sparse and time-varying coefficient process in the high-dimensional set-up. Specifically, to account for the sparse and time-varying coefficient process, we applied the Dantzig procedure to the instantaneous coefficient estimator, which results in a biased estimator. To reduce the bias, we proposed a debiased estimation procedure. We estimated the integrated coefficient with this new debiased instantaneous coefficient estimator. We showed that the Dantzig procedure can handle the sparsity of the instantaneous coefficient and that the debiased scheme mitigates the errors from the bias of the instantaneous coefficient estimator. To accommodate the sparsity of the integrated coefficient, we further regularized the coefficient estimator. Finally, we showed that the proposed TED estimator can obtain the near-optimal convergence rate.

In the empirical study, the TED estimator outperforms other estimators in terms of predictive accuracy in out-of-sample analysis. Furthermore, we found that the coefficient process is sparse and time-varying. These findings revealed that, when analyzing high-dimensional high-frequency regression, the TED estimator is a useful tool that can handle the curse of dimensionality and time-varying coefficients. That is, in practice, the TED procedure makes it possible to analyze the stock market with a relatively short period using high-frequency data.

Statistical inference—hypothesis tests or confidence intervals—on the integrated coefficient estimator is also important and essential. However, under the current debiasing scheme, the sum of non-martingale terms,  $R_i$ , is not negligible compared to the sum of martingale terms, which makes inference infeasible. To solve this issue, we may need to develop a novel debiasing scheme for the biased integrated coefficient estimator. This is a demand-

ing task. On the other hand, high-dimensional covariates often exhibit a factor structure, which can be addressed using a PCA-based approach. However, applying this more elaborate model within a simple framework introduces substantial estimation error, which outweighs the benefits of alleviating model misspecification. An interesting avenue for future work is to develop a method that explicitly incorporates the factor structure of covariate processes while providing a clearer explanation of market dynamics. We leave these issues for future research.

## Disclosure statement

The authors report there are no competing interests to declare.

## Data availability statement

The data that support the findings of this study are available from the End of Day website (<https://eoddata.com>), firm fundamentals from the Center for Research in Security Prices (CRSP)/Compustat Merged Database, and the high-frequency factor returns from <https://www.sakethaleti.com/data>.

## References

- Aït-Sahalia, Y., Kalnina, I., and Xiu, D. (2020). High-frequency factor models and regressions. *Journal of Econometrics*, 216(1):86–105.
- Aït-Sahalia, Y. and Xiu, D. (2017). Using principal component analysis to estimate a high dimensional factor model with high-frequency data. *Journal of Econometrics*, 201(2):384–399.

- Aït-Sahalia, Y. and Xiu, D. (2019a). A hausman test for the presence of market microstructure noise in high frequency data. *Journal of Econometrics*, 211(1):176–205.
- Aït-Sahalia, Y. and Xiu, D. (2019b). Principal component analysis of high-frequency data. *Journal of the American Statistical Association*, 114(525):287–303.
- Aleti, S. (2022). The high-frequency factor zoo. *Available at SSRN 4021620*.
- Andersen, T. G., Thyrgaard, M., and Todorov, V. (2021). Recalcitrant betas: Intraday variation in the cross-sectional dispersion of systematic risk. *Quantitative Economics*, 12(2):647–682.
- Ang, A. and Kristensen, D. (2012). Testing conditional factor models. *Journal of Financial Economics*, 106(1):132–156.
- Asness, C. S., Moskowitz, T. J., and Pedersen, L. H. (2013). Value and momentum everywhere. *The Journal of Finance*, 68(3):929–985.
- Barndorff-Nielsen, O. E., Hansen, P. R., Lunde, A., and Shephard, N. (2011). Multivariate realised kernels: consistent positive semi-definite estimators of the covariation of equity prices with noise and non-synchronous trading. *Journal of Econometrics*, 162(2):149–169.
- Barroso, P. and Santa-Clara, P. (2015). Momentum has its moments. *Journal of Financial Economics*, 116(1):111–120.
- Belloni, A., Chernozhukov, V., and Hansen, C. (2014). Inference on treatment effects after selection among high-dimensional controls. *The Review of Economic Studies*, 81(2):608–650.
- Bickel, P. J. and Levina, E. (2008). Covariance regularization by thresholding. *The Annals of Statistics*, pages 2577–2604.

- Bickel, P. J., Ritov, Y., and Tsybakov, A. B. (2009). Simultaneous analysis of LASSO and Dantzig selector. *The Annals of Statistics*, 37(4):1705–1732.
- Boyd, S. P. and Vandenberghe, L. (2004). *Convex optimization*. Cambridge university press.
- Cai, T. and Liu, W. (2011). Adaptive thresholding for sparse covariance matrix estimation. *Journal of the American Statistical Association*, 106(494):672–684.
- Cai, T., Liu, W., and Luo, X. (2011). A constrained  $\ell_1$  minimization approach to sparse precision matrix estimation. *Journal of the American Statistical Association*, 106(494):594–607.
- Cai, T. T. and Zhou, H. H. (2012). Optimal rates of convergence for sparse covariance matrix estimation. *The Annals of Statistics*, 40(5):2389 – 2420.
- Candes, E. and Tao, T. (2007). The dantzig selector: Statistical estimation when  $p$  is much larger than  $n$ . *The Annals of Statistics*, 35(6):2313–2351.
- Carhart, M. M. (1997). On persistence in mutual fund performance. *The Journal of Finance*, 52(1):57–82.
- Chen, D., Mykland, P. A., and Zhang, L. (2024). Realized regression with asynchronous and noisy high frequency and high dimensional data. *Journal of Econometrics*, 239(2):105446.
- Chen, R. Y. (2018). Inference for volatility functionals of multivariate Itô semimartingales observed with jump and noise. *arXiv preprint arXiv:1810.04725*.
- Ciolek, G., Marushkevych, D., and Podolskij, M. (2022). On lasso estimator for the drift function in diffusion models. *arXiv preprint arXiv:2209.05974*.
- Cochrane, J. H. (2011). Presidential address: Discount rates. *The Journal of Finance*, 66(4):1047–1108.
- Fama, E. F. and French, K. R. (1997). Industry costs of equity. *Journal of Financial Economics*, 43(2):153–193.



- Fama, E. F. and French, K. R. (2015). A five-factor asset pricing model. *Journal of Financial Economics*, 116(1):1–22.
- Fama, E. F. and French, K. R. (2016). Dissecting anomalies with a five-factor model. *The Review of Financial Studies*, 29(1):69–103.
- Fan, J. and Kim, D. (2018). Robust high-dimensional volatility matrix estimation for high-frequency factor model. *Journal of the American Statistical Association*, 113(523):1268–1283.
- Fan, J., Li, Q., and Wang, Y. (2017). Estimation of high dimensional mean regression in the absence of symmetry and light tail assumptions. *Journal of the Royal Statistical Society Series B: Statistical Methodology*, 79(1):247–265.
- Fan, J. and Li, R. (2001). Variable selection via nonconcave penalized likelihood and its oracle properties. *Journal of the American Statistical Association*, 96(456):1348–1360.
- Fan, J., Liao, Y., and Mincheva, M. (2013). Large covariance estimation by thresholding principal orthogonal complements. *Journal of the Royal Statistical Society: Series B (Statistical Methodology)*, 75(4):603–680.
- Feng, G., Giglio, S., and Xiu, D. (2020). Taming the factor zoo: A test of new factors. *The Journal of Finance*, 75(3):1327–1370.
- Gaïffas, S. and Matulewicz, G. (2019). Sparse inference of the drift of a high-dimensional ornstein–uhlenbeck process. *Journal of Multivariate Analysis*, 169:1–20.
- Harvey, C. R., Liu, Y., and Zhu, H. (2016). ... and the cross-section of expected returns. *The Review of Financial Studies*, 29(1):5–68.
- Hou, K., Xue, C., and Zhang, L. (2020). Replicating anomalies. *The Review of Financial Studies*, 33(5):2019–2133.

- Jacod, J. and Protter, P. E. (2011). *Discretization of processes*, volume 67. Springer Science & Business Media.
- Javanmard, A. and Montanari, A. (2018). Debiasing the lasso: Optimal sample size for gaussian designs. *The Annals of Statistics*, 46(6A):2593–2622.
- Jensen, T. I., Kelly, B., and Pedersen, L. H. (2023). Is there a replication crisis in finance? *The Journal of Finance*, 78(5):2465–2518.
- Kim, D., Kong, X.-B., Li, C.-X., and Wang, Y. (2018). Adaptive thresholding for large volatility matrix estimation based on high-frequency financial data. *Journal of Econometrics*, 203(1):69–79.
- Kim, D. and Wang, Y. (2016). Sparse PCA-based on high-dimensional Itô processes with measurement errors. *Journal of Multivariate Analysis*, 152:172–189.
- Kim, D., Wang, Y., and Zou, J. (2016). Asymptotic theory for large volatility matrix estimation based on high-frequency financial data. *Stochastic Processes and their Applications*, 126:3527–3577.
- McLean, R. D. and Pontiff, J. (2016). Does academic research destroy stock return predictability? *The Journal of Finance*, 71(1):5–32.
- Mykland, P. A. and Zhang, L. (2009). Inference for continuous semimartingales observed at high frequency. *Econometrica*, 77(5):1403–1445.
- Negahban, S. N., Ravikumar, P., Wainwright, M. J., and Yu, B. (2012). A unified framework for high-dimensional analysis of  $m$ -estimators with decomposable regularizers. *Statistical Science*, 27(4):538–557.
- Oh, M., Kim, D., and Wang, Y. (2024). Robust realized integrated beta estimator with application to dynamic analysis of integrated beta. *Journal of Econometrics*, page 105810.

- Pang, H., Liu, H., and Vanderbei, R. J. (2014). The fastclime package for linear programming and large-scale precision matrix estimation in r. *Journal of Machine Learning Research*.
- Park, T. and Casella, G. (2008). The bayesian lasso. *Journal of the American Statistical Association*, 103(482):681–686.
- Shin, M. and Kim, D. (2023). Robust high-dimensional time-varying coefficient estimation. *arXiv preprint arXiv:2302.13658*.
- Tao, M., Wang, Y., and Zhou, H. H. (2013). Optimal sparse volatility matrix estimation for high-dimensional Itô processes with measurement errors. *The Annals of Statistics*, 41(4):1816–1864.
- Tibshirani, R. (1996). Regression shrinkage and selection via the lasso. *Journal of the Royal Statistical Society: Series B (Methodological)*, 58(1):267–288.
- Van de Geer, S., Bühlmann, P., Ritov, Y., and Dezeure, R. (2014). On asymptotically optimal confidence regions and tests for high-dimensional models. *The Annals of Statistics*, 42(3):1166–1202.
- Wang, Y. and Zou, J. (2010). Vast volatility matrix estimation for high-frequency financial data. *The Annals of Statistics*, 38:943–978.
- Yuan, M. and Lin, Y. (2006). Model selection and estimation in regression with grouped variables. *Journal of the Royal Statistical Society: Series B (Statistical Methodology)*, 68(1):49–67.
- Zhang, C.-H. and Zhang, S. S. (2014). Confidence intervals for low dimensional parameters in high dimensional linear models. *Journal of the Royal Statistical Society Series B: Statistical Methodology*, 76(1):217–242.

- Zhang, L. (2011). Estimating covariation: Epps effect, microstructure noise. *Journal of Econometrics*, 160(1):33–47.
- Zou, H. (2006). The adaptive lasso and its oracle properties. *Journal of the American Statistical Association*, 101(476):1418–1429.
- Zou, H. and Hastie, T. (2005). Regularization and variable selection via the elastic net. *Journal of the Royal Statistical Society Series B: Statistical Methodology*, 67(2):301–320.
- Zou, H. and Zhang, H. H. (2009). On the adaptive elastic-net with a diverging number of parameters. *The Annals of Statistics*, 37(4):1733.

# Appendix

## A Implementation details of TED

In this section, we provide implementation details of the TED procedure, including the pseudocode in Algorithm 2, graphical illustration in Figure 5, and computational complexity analyses. Specifically, Figure 5 illustrates the TED procedure with simulation data in Section 4. The first panel displays the instantaneous coefficient  $\widehat{\beta}_0$  estimates obtained through the Dantzig selector. We used the “dantzig” function in the fastclime package in R (Pang et al., 2014). The second panel shows the bias adjustment term, distinguishing between positive (blue) and negative (red) biases to debias the instantaneous coefficient. For the CLIME estimator, we employed the “fastclime” function in the fastclime package. The third panel presents the debiased instantaneous coefficient  $\widetilde{\beta}_0$  estimates, which are obtained by summing the estimates from the first two panels. The fourth panel illustrates the iteratively calculated debiased instantaneous coefficient estimates over time. The fifth panel shows the integrated coefficient estimates  $\widehat{I\beta}$ , which is the integral of the debiased instantaneous coefficient estimates. Finally, the last panel displays the TED estimates  $\widetilde{I\beta}$  after applying thresholding to the integrated coefficient estimates.

When it comes to practical use, the time complexity of the TED procedure becomes an important consideration. For the TED procedure, the most computationally intensive part is estimating the inverse covariance matrix using the CLIME estimator (Cai et al., 2011). The CLIME estimator solves the following optimization problem:

$$\min \|\Omega\|_1 \quad \text{s.t.} \quad \|\Sigma\Omega - \mathbf{I}\|_{\max} \leq \tau_n,$$

---

**Algorithm 2** TED pseudocode.

---

```

1: function TED
2:   input: High frequency data  $(\Delta_i^n Y, \Delta_i^n \mathbf{X})_{i=1,\dots,n}$ , tuning parameters  $(k_n, \lambda_n, \tau_n, h_n)$ ,
   thresholding function  $s(\cdot)$ ;
3:    $N \leftarrow \lfloor 1/(k_n \Delta_n) \rfloor$ ;
4:   for  $i = 0, 1, \dots, N-1$  do
5:      $\mathcal{Y}_{ik_n} \leftarrow (\Delta_{ik_n+1}^n Y, \Delta_{ik_n+2}^n Y, \dots, \Delta_{(i+1)k_n}^n Y)^\top$ ;
6:      $\mathcal{X}_{ik_n} \leftarrow (\Delta_{ik_n+1}^n \mathbf{X}, \Delta_{ik_n+2}^n \mathbf{X}, \dots, \Delta_{(i+1)k_n}^n \mathbf{X})^\top$ ;
7:      $\hat{\Sigma}_{ik_n \Delta_n} \leftarrow \frac{1}{k_n \Delta_n} \mathcal{X}_{ik_n}^\top \mathcal{X}_{ik_n}$ ;
8:      $\hat{\Sigma}_{XY, ik_n \Delta_n} \leftarrow \frac{1}{k_n \Delta_n} \mathcal{X}_{ik_n}^\top \mathcal{Y}_{ik_n}$ ;
9:      $\hat{\beta}_{ik_n \Delta_n} \leftarrow \arg \min_{\beta} \|\beta\|_1 \quad \text{s.t.} \quad \left\| \hat{\Sigma}_{ik_n \Delta_n} \beta - \hat{\Sigma}_{XY, ik_n \Delta_n} \right\|_{\max} \leq \lambda_n$ ;
10:     $\hat{\Omega}_{ik_n \Delta_n} \leftarrow \arg \min_{\Omega} \|\Omega\|_1 \quad \text{s.t.} \quad \left\| \hat{\Sigma}_{ik_n \Delta_n} \Omega - \mathbf{I} \right\|_{\max} \leq \tau_n$ ;
11:     $\tilde{\beta}_{ik_n \Delta_n} \leftarrow \hat{\beta}_{ik_n \Delta_n} + \hat{\Omega}_{ik_n \Delta_n}^\top \left( \hat{\Sigma}_{XY, ik_n \Delta_n} - \hat{\Sigma}_{ik_n \Delta_n} \hat{\beta}_{ik_n \Delta_n} \right)$ ;
12:  end for
13:   $\widehat{I\beta} \leftarrow \sum_{i=0}^{N-1} \tilde{\beta}_{ik_n \Delta_n} k_n \Delta_n$ ;
14:  for  $i = 1, \dots, p$  do
15:     $\widetilde{I\beta}_i \leftarrow s(\widehat{I\beta}_i) \mathbf{1}(|\widehat{I\beta}_i| \geq h_n)$ ;
16:  end for
17:  Output:  $\widetilde{I\beta} \leftarrow (\widetilde{I\beta}_i)_{i=1,\dots,p}$ ;
18: end function

```

---

where  $\Sigma = \frac{1}{k_n \Delta_n} \mathcal{X}_i^\top \mathcal{X}_i$ . The above optimization problem is equivalent to solving

$$\begin{aligned}
\min (\Omega_{\cdot i}^+ + \Omega_{\cdot i}^-)^\top \mathbf{1} \quad \text{s.t.} \quad & \begin{pmatrix} \Sigma & -\Sigma \\ -\Sigma & \Sigma \end{pmatrix} \begin{pmatrix} \Omega_{\cdot i}^+ \\ \Omega_{\cdot i}^- \end{pmatrix} \leq \begin{pmatrix} \tau_n \mathbf{1} + e_i \\ \tau_n \mathbf{1} - e_i \end{pmatrix} \\
& \Omega_{\cdot i}^+ \geq 0, \quad \text{and} \quad \Omega_{\cdot i}^- \geq 0,
\end{aligned} \tag{A.1}$$

for each  $i = 1, \dots, p$  (Cai et al., 2011). Using a primal-dual interior point method (Boyd and Vandenberghe, 2004), each linear program can be solved in  $O(p^3 \times \sqrt{p} \log p)$  time. Therefore, the total computational cost for estimating the inverse covariance matrix is  $O(p^4 \sqrt{p} \log p)$  time. Dantzig selector (3.3) can be solved similarly using a primal-dual interior point method, but since there is only one optimization problem per time-localized window, the time complexity is  $O(p^3 \sqrt{p} \log p)$ . Since there are  $O(n^{1/2})$  time-localized windows, the total time

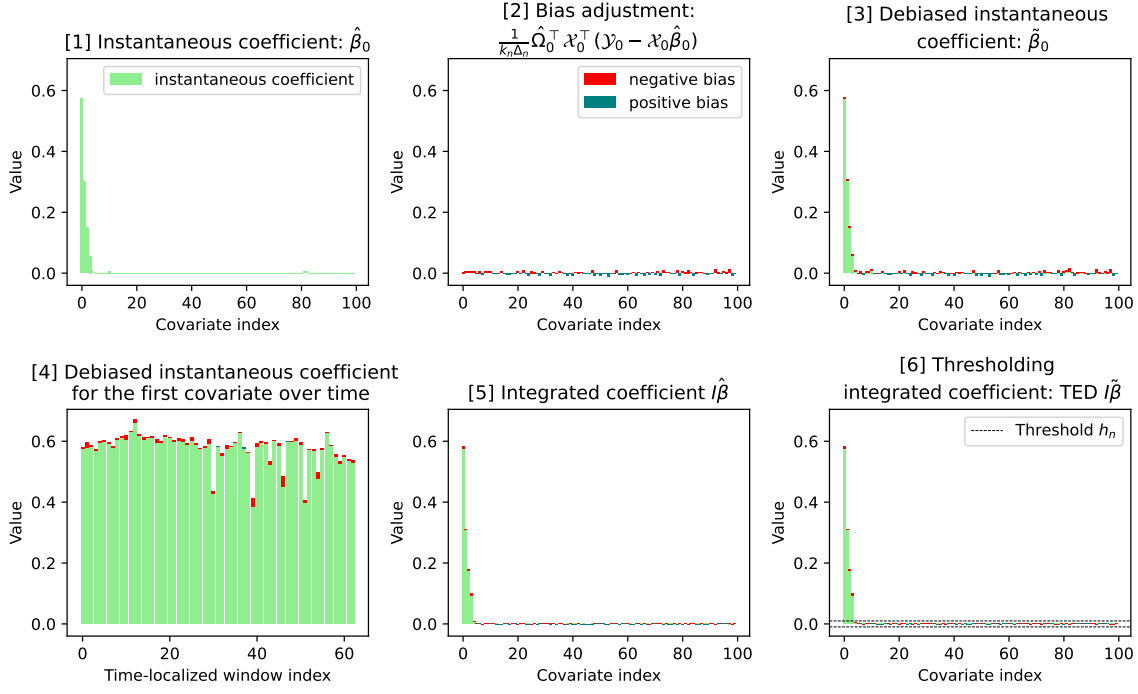


Figure 5: Graphical illustration of the TED procedure.

complexity for the TED procedure is  $O(n^{1/2}p^4\sqrt{p}\log p)$ . Space complexity for the TED procedure is  $O(p^2)$ . Therefore, the TED procedure can be implemented in polynomial time and space in terms of  $p$  and  $n$ .

If  $p$  is so large that the time complexity of TED is a critical issue in the application, we can use an alternative inverse covariance matrix estimator, such as Principal Orthogonal complement Thresholding (POET) (Fan et al., 2013), or parallelize the TED procedure. The POET procedure requires  $O(p^2r)$  time to compute the covariance and  $O(p^3)$  time to compute the algebraic inverse, where  $r$  is the number of common factors. In this case, the total time complexity for the TED procedure becomes  $O(n^{1/2}p^3\sqrt{p}\log p)$ .

Alternatively, we can parallelize the TED procedure by computing each instantaneous coefficient independently. Suppose  $M$  processors are available. Then, the total time complexity can be reduced to  $O(n^{1/2}M^{-1}p^4\sqrt{p}\log p + p^4\sqrt{p}\log p)$ . When the number of processors  $M$  is large enough, specifically  $M \gg n^{1/2}$ , parallelizing the instantaneous coefficient estimations becomes inefficient. In this case, it is preferable to parallelize the CLIME estimator, which is

the most computationally intensive part of the instantaneous coefficient estimation. Specifically, since each linear program (A.1) can be solved independently, the CLIME estimator can be efficiently parallelized. Then, each instantaneous coefficient estimator can be computed in  $O(M^{-1}p^4\sqrt{p}\log p + p^3\sqrt{p}\log p)$  time. In this case, the total time complexity becomes  $O(n^{1/2}p^4M^{-1}\sqrt{p}\log p + n^{1/2}p^3\sqrt{p}\log p)$ .

## B Conditions for extension of TED

Empirical data often exhibit specific features, such as microstructure noise or heavy-tailed distributions, that require robust estimation techniques. While the TED procedure effectively handles high-dimensional and time-varying coefficients under regular conditions, practical applications might involve these additional complexities. If we can estimate instantaneous covariances with certain convergence rates, then we can directly utilize the TED framework by replacing the instantaneous covariance estimators  $\frac{1}{k_n\Delta_n}\mathcal{X}_i^\top\mathcal{X}_i$  and  $\frac{1}{k_n\Delta_n}\mathcal{X}_i^\top\mathcal{Y}_i$  with proper robust estimators  $\widehat{\Sigma}_{ik_n\Delta_n}$  and  $\widehat{\Sigma}_{XY,ik_n\Delta_n}$ , respectively. The instantaneous covariance estimators should satisfy the following error bounds with high probability:

$$\begin{aligned} \left\| \widehat{\Sigma}_{ik_n\Delta_n} - \Sigma_{ik_n\Delta_n} \right\|_{\max} &\leq Cn^{-1/4}\sqrt{\log p} \quad \text{and} \\ \left\| \widehat{\Sigma}_{ik_n\Delta_n}\beta_{ik_n\Delta_n} - \widehat{\Sigma}_{XY,ik_n\Delta_n} \right\|_{\max} &\leq Cs_p n^{-1/4}\sqrt{\log p}. \end{aligned} \quad (\text{B.1})$$

The first error is related to the estimation of the instantaneous covariance matrix  $\Sigma_{ik_n\Delta_n}$ . The second error is associated with the smooth time-varying coefficient and the tail behavior of the residual process. To robustly handle these empirical features, we can follow the ideas of Aït-Sahalia and Xiu (2017); Barndorff-Nielsen et al. (2011); Fan and Kim (2018); Kim et al. (2018); Shin and Kim (2023); Zhang (2011). Under Assumption 1, we can show that the instantaneous covariance estimators  $\frac{1}{k_n\Delta_n}\mathcal{X}_i^\top\mathcal{X}_i$  and  $\frac{1}{k_n\Delta_n}\mathcal{X}_i^\top\mathcal{Y}_i$  used in the TED procedure satisfy the error bounds (B.1). See (C.7) for details.



## C Proofs

### C.1 Proofs of Theorems 1 and 2

Without loss of generality, it is enough to show the statements of Theorems 1 and 2 for fixed  $i$ .

**Proof of Theorem 1.** We denote the true instantaneous coefficient at time  $i\Delta_n$  by  $\beta_0$ . We have

$$\begin{aligned}\Delta_{i+k}^n Y &= \int_{(i+k-1)\Delta_n}^{(i+k)\Delta_n} \beta_t^\top d\mathbf{X}_t + \int_{(i+k-1)\Delta_n}^{(i+k)\Delta_n} dZ_t \\ &= \beta_0^\top \Delta_{i+k}^n \mathbf{X} + \Delta_{i+k}^n Z + \int_{(i+k-1)\Delta_n}^{(i+k)\Delta_n} (\beta_t - \beta_0)^\top d\mathbf{X}_t.\end{aligned}$$

Then, we have

$$\mathcal{Y}_i = \mathcal{X}_i \beta_0 + \mathcal{Z}_i + \tilde{\mathcal{X}}_i, \quad (\text{C.1})$$

where

$$\tilde{\mathcal{X}}_i = \begin{pmatrix} \int_{i\Delta_n}^{(i+1)\Delta_n} (\beta_t - \beta_0)^\top d\mathbf{X}_t \\ \int_{(i+1)\Delta_n}^{(i+2)\Delta_n} (\beta_t - \beta_0)^\top d\mathbf{X}_t \\ \vdots \\ \int_{(i+k_n-1)\Delta_n}^{(i+k_n)\Delta_n} (\beta_t - \beta_0)^\top d\mathbf{X}_t \end{pmatrix}.$$

Since the instantaneous volatility and drift processes are bounded,  $\Delta_{i+k}^n Z$  and  $\Delta_{i+k}^n X_j$  are sub-Gaussian. Then, similar to the proof of Theorem 1 (Kim and Wang, 2016), we can show, for some large  $C$ ,

$$P \left( \max_{1 \leq j \leq p} \left| \frac{1}{k_n \Delta_n} \sum_{k=0}^{k_n} \Delta_{i+k}^n Z \Delta_{i+k}^n X_j \right| \geq C \sqrt{\log p / k_n} \right) \leq p^{-1-a}, \quad (\text{C.2})$$

where  $X_j$  is the  $j$ th element of  $\mathbf{X}$ .

Consider  $\frac{1}{k_n \Delta_n} \mathcal{X}_i^\top \tilde{\mathcal{X}}_i$ . There exist standard Brownian motions,  $W_{mt}^*$  and  $B_{it}^*$ , such that

$$d\beta_{mt} = \mu_{\beta,mt}dt + \sqrt{\Sigma_{\beta,mmt}}dW_{mt}^* \quad \text{and} \quad dX_{it} = \mu_{it}dt + \sqrt{\Sigma_{iit}}dB_{it}^*,$$

and let  $\tilde{X}_{mt} = \int_{i\Delta_n}^t (\beta_{ms} - \beta_{m0})dX_{ms}$ . By Itô's formula, we have

$$\begin{aligned} & \int_{(i+k-1)\Delta_n}^{(i+k)\Delta_n} dX_{jt} \int_{(i+k-1)\Delta_n}^{(i+k)\Delta_n} (\beta_{mt} - \beta_{m0})dX_{mt} \\ &= \int_{(i+k-1)\Delta_n}^{(i+k)\Delta_n} (\beta_{mt} - \beta_{m0})\Sigma_{jmt}dt \\ & \quad + \int_{(i+k-1)\Delta_n}^{(i+k)\Delta_n} (\tilde{X}_{mt} - \tilde{X}_{m(i+k-1)\Delta_n})dX_{jt} + \int_{(i+k-1)\Delta_n}^{(i+k)\Delta_n} (X_{jt} - X_{j(i+k-1)\Delta_n})d\tilde{X}_{mt} \\ &= \int_{(i+k-1)\Delta_n}^{(i+k)\Delta_n} \int_{i\Delta_n}^t \sqrt{\Sigma_{\beta,mmt}}dW_{ms}^* \Sigma_{jmt}dt + \int_{(i+k-1)\Delta_n}^{(i+k)\Delta_n} \int_{i\Delta_n}^t \mu_{\beta,ms}ds \Sigma_{jmt}dt \\ & \quad + \int_{(i+k-1)\Delta_n}^{(i+k)\Delta_n} (\tilde{X}_{mt} - \tilde{X}_{m(i+k-1)\Delta_n})\sqrt{\Sigma_{jjt}}dB_{jt}^* + \int_{(i+k-1)\Delta_n}^{(i+k)\Delta_n} (\tilde{X}_{mt} - \tilde{X}_{m(i+k-1)\Delta_n})\mu_{jt}dt \\ & \quad + \int_{(i+k-1)\Delta_n}^{(i+k)\Delta_n} (X_{jt} - X_{j(i+k-1)\Delta_n})\sqrt{\Sigma_{mmt}}(\beta_{mt} - \beta_{m0})dB_{mt}^* \\ & \quad + \int_{(i+k-1)\Delta_n}^{(i+k)\Delta_n} (X_{jt} - X_{j(i+k-1)\Delta_n})(\beta_{mt} - \beta_{m0})\mu_{mt}dt \\ &= M_{1km} + D_{1km} + M_{2km} + D_{2km} + M_{3km} + D_{3km} \text{ a.s.} \end{aligned}$$

First, consider  $D_{ikm}$ 's. By Assumption 1(b)–(c), we have

$$\left| \frac{1}{k_n \Delta_n} \sum_{m=1}^p \sum_{k=1}^{k_n} D_{1km} \right| \leq C s_p k_n \Delta_n \text{ a.s.}$$

For  $D_{2km}$ , by Assumption 1(b)–(c), the process  $\sum_{m=1}^p |\beta_{mt} - \beta_{m0}|$  has the sub-Gaussian tail and  $\sum_{m=1}^p \sqrt{\Sigma_{\beta,mmt}} \leq C \sum_{m=1}^p |\Sigma_{\beta,mmt}|^{\delta/2} \leq C s_p$ . Thus, we can show

$$\begin{aligned} & P \left( \sup_{t \in [i\Delta_n, (i+k_n)\Delta_n]} \sum_{m=1}^p |\beta_{mt} - \beta_{m0}| \geq C s_p \sqrt{\Delta_n k_n \log p} \right) \\ & \leq C P \left( \sum_{m=1}^p |\beta_{m(i+k_n)\Delta_n} - \beta_{m0}| \geq C s_p \sqrt{\Delta_n k_n \log p} \right) \\ & \leq p^{-3-a-c/c_1}. \end{aligned} \tag{C.3}$$

Let

$$E = \left\{ \sup_{t \in [i\Delta_n, (i+k_n)\Delta_n]} \sum_{m=1}^p |\beta_{mt} - \beta_{m0}| \geq C s_p \sqrt{\Delta_n k_n \log p} \right\}.$$

Then, we have

$$\begin{aligned} & P \left( \sup_{t \in [(i+k-1)\Delta_n, (i+k)\Delta_n]} \sum_{m=1}^p |\tilde{X}_{mt} - \tilde{X}_{m(i+k-1)\Delta_n}| \geq C s_p \log p \sqrt{\Delta_n^2 k_n} \right) \\ & \leq CP \left( \sum_{m=1}^p |\tilde{X}_{m(i+k)\Delta_n} - \tilde{X}_{m(i+k-1)\Delta_n}| \geq C s_p \log p \sqrt{\Delta_n^2 k_n} \right) \\ & \leq CP \left( \sum_{m=1}^p \left| \int_{(i+k-1)\Delta_n}^{(i+k)\Delta_n} (\beta_{mt} - \beta_{m0}) dX_{mt} \right| \geq C s_p \log p \sqrt{\Delta_n^2 k_n}, E^c \right) + p^{-3-a-c/c_1} \\ & \leq Cp^{-3-a-c/c_1}, \end{aligned}$$

which implies

$$P \left( \sup_{1 \leq k \leq k_n} \sup_{t \in [(i+k-1)\Delta_n, (i+k)\Delta_n]} \sum_{m=1}^p |\tilde{X}_{mt} - \tilde{X}_{m(i+k-1)\Delta_n}| \geq C s_p \log p \sqrt{\Delta_n^2 k_n} \right) \leq Cp^{-3-a}. \quad (\text{C.4})$$

Thus, we have, with probability at least  $1 - p^{-2-a}$ ,

$$\left| \frac{1}{k_n \Delta_n} \sum_{m=1}^p \sum_{k=1}^{k_n} D_{2km} \right| \leq C s_p \log p \sqrt{\Delta_n^2 k_n}.$$

Similarly, we can show, with probability at least  $1 - p^{-2-a}$ ,

$$\left| \frac{1}{k_n \Delta_n} \sum_{m=1}^p \sum_{k=1}^{k_n} D_{3km} \right| \leq C s_p \log p \sqrt{\Delta_n^2 k_n}.$$

Consider  $M_{ikm}$ 's. By Azuma-Hoeffding inequality, we have, with probability at least  $1 - p^{-2-a}$ ,

$$\left| \frac{1}{k_n \Delta_n} \sum_{m=1}^p \sum_{k=1}^{k_n} M_{1km} \right| \leq C s_p \sqrt{\Delta_n k_n \log p}.$$

For  $M_{2km}$ , let

$$\eta_{mt} = (\tilde{X}_{mt} - \tilde{X}_{m(i+k-1)\Delta_n})\sqrt{\Sigma_{jjt}} \quad \text{and} \quad Q_t = \mathbf{1}_{\{\sum_{m=1}^p |\eta_{mt}| \leq C s_p \log p \sqrt{\Delta_n^2 k_n}\}}.$$

Then, by Azuma-Hoeffding inequality, we have, with probability at least  $1 - p^{-3-a}$ ,

$$\left| \frac{1}{k_n \Delta_n} \sum_{m=1}^p \sum_{k=1}^{k_n} \int_{(i+k-1)\Delta_n}^{(i+k)\Delta_n} \eta_{mt} Q_t dB_{jt}^* \right| \leq C s_p \sqrt{\Delta_n} (\log p)^{3/2}.$$

Thus, by (C.4), we have, with probability at least  $1 - p^{-2-a}$ ,

$$\left| \frac{1}{k_n \Delta_n} \sum_{m=1}^p \sum_{k=1}^{k_n} M_{2km} \right| \leq C s_p \sqrt{\Delta_n} (\log p)^{3/2}.$$

Similarly, we can show, with probability at least  $1 - p^{-2-a}$ ,

$$\left| \frac{1}{k_n \Delta_n} \sum_{m=1}^p \sum_{k=1}^{k_n} M_{3km} \right| \leq C s_p \sqrt{\Delta_n} (\log p)^{3/2}.$$

Therefore, we have, with probability at least  $1 - Cp^{-1-a}$ ,

$$\begin{aligned} & \max_{1 \leq j \leq p} \left| \frac{1}{k_n \Delta_n} \sum_{k=1}^{k_n} \Delta_{i+k}^n X_j \int_{(i+k-1)\Delta_n}^{(i+k)\Delta_n} (\beta_t - \beta_0)^\top d\mathbf{X}_t \right| \\ & \leq C s_p \sqrt{\Delta_n k_n \log p}. \end{aligned} \tag{C.5}$$

With probability greater than  $1 - p^{-1-a}$ , we have

$$\begin{aligned} \left\| \frac{d}{dt} [\mathbf{X}, \mathbf{X}]_{i\Delta_n} - \frac{1}{k_n \Delta_n} \mathcal{X}_i^\top \mathcal{X}_i \right\|_{\max} & \leq \left\| \Sigma_{i\Delta_n} - \frac{1}{k_n \Delta_n} \int_{i\Delta_n}^{(i+k_n)\Delta_n} \Sigma_s ds \right\|_{\max} \\ & \quad + \left\| \frac{1}{k_n \Delta_n} \int_{i\Delta_n}^{(i+k_n)\Delta_n} \Sigma_s ds - \frac{1}{k_n \Delta_n} \mathcal{X}_i^\top \mathcal{X}_i \right\|_{\max} \\ & \leq C \sqrt{k_n \Delta_n} + C \sqrt{\log p / k_n}, \end{aligned} \tag{C.6}$$

where  $\frac{d}{dt}[\mathbf{X}, \mathbf{X}]_t = \boldsymbol{\Sigma}_t$  and the last inequality can be showed similar to the proofs of Theorem 1 (Kim and Wang, 2016). Thus, by (C.2), (C.5), and (C.6), we show the statement under the following statements:

$$\begin{aligned} \left\| \frac{1}{k_n \Delta_n} \mathcal{X}_i^\top \mathcal{Z}_i \right\|_{\max} &\leq C \sqrt{\log p / k_n}, \\ \left\| \frac{1}{k_n \Delta_n} \mathcal{X}_i^\top \tilde{\mathcal{X}}_i \right\|_{\max} &\leq C s_p \sqrt{k_n \Delta_n} \sqrt{\log p}, \\ \left\| \frac{d}{dt} [\mathbf{X}, \mathbf{X}]_{i \Delta_n} - \frac{1}{k_n \Delta_n} \mathcal{X}_i^\top \mathcal{X}_i \right\|_{\max} &\leq C (\sqrt{k_n \Delta_n} + \sqrt{\log p / k_n}). \end{aligned} \quad (\text{C.7})$$

By (C.7), we have, for some large  $C_{\lambda, a}$ ,

$$\begin{aligned} &\left\| \frac{1}{k_n \Delta_n} \mathcal{X}_i^\top \mathcal{X}_i \boldsymbol{\beta}_0 - \frac{1}{k_n \Delta_n} \mathcal{X}_i^\top \mathcal{Y}_i \right\|_{\max} \\ &= \left\| \frac{1}{k_n \Delta_n} \mathcal{X}_i^\top \mathcal{X}_i \boldsymbol{\beta}_0 - \frac{1}{k_n \Delta_n} \mathcal{X}_i^\top \mathcal{X}_i \boldsymbol{\beta}_0 - \frac{1}{k_n \Delta_n} \mathcal{X}_i^\top \mathcal{Z}_i - \frac{1}{k_n \Delta_n} \mathcal{X}_i^\top \tilde{\mathcal{X}}_i \right\|_{\max} \\ &\leq \left\| \frac{1}{k_n \Delta_n} \mathcal{X}_i^\top \mathcal{Z}_i \right\|_{\max} + \left\| \frac{1}{k_n \Delta_n} \mathcal{X}_i^\top \tilde{\mathcal{X}}_i \right\|_{\max} \\ &\leq \lambda_n. \end{aligned}$$

Thus,  $\boldsymbol{\beta}_0$  satisfies the constraint in (3.3), which implies that

$$\|\hat{\boldsymbol{\beta}}_{i \Delta_n}\|_1 \leq \|\boldsymbol{\beta}_0\|_1.$$

We have

$$\begin{aligned} \left\| \frac{1}{k_n \Delta_n} \mathcal{X}_i^\top \mathcal{X}_i (\hat{\boldsymbol{\beta}}_{i \Delta_n} - \boldsymbol{\beta}_0) \right\|_{\max} &\leq \left\| \frac{1}{k_n \Delta_n} \mathcal{X}_i^\top \mathcal{X}_i \hat{\boldsymbol{\beta}}_{i \Delta_n} - \frac{1}{k_n \Delta_n} \mathcal{X}_i^\top \mathcal{Y}_i \right\|_{\max} \\ &\quad + \left\| \frac{1}{k_n \Delta_n} \mathcal{X}_i^\top \mathcal{X}_i \boldsymbol{\beta}_0 - \frac{1}{k_n \Delta_n} \mathcal{X}_i^\top \mathcal{Y}_i \right\|_{\max} \\ &\leq 2\lambda_n \end{aligned}$$

and

$$\begin{aligned}
\|\Sigma_{i\Delta_n}(\widehat{\beta}_{i\Delta_n} - \beta_0)\|_{\max} &\leq \left\| \frac{1}{k_n\Delta_n} \mathcal{X}_i^\top \mathcal{X}_i (\widehat{\beta}_{i\Delta_n} - \beta_0) \right\|_{\max} \\
&\quad + \left\| \left( \Sigma_{i\Delta_n} - \frac{1}{k_n\Delta_n} \mathcal{X}_i^\top \mathcal{X}_i \right) (\widehat{\beta}_{i\Delta_n} - \beta_0) \right\|_{\max} \\
&\leq 2\lambda_n + 2\|\beta_0\|_1 \left\| \Sigma_{i\Delta_n} - \frac{1}{k_n\Delta_n} \mathcal{X}_i^\top \mathcal{X}_i \right\|_{\max} \\
&\leq 2\lambda_n + C s_p (\sqrt{k_n\Delta_n} + \sqrt{\log p/k_n}) \\
&\leq C\lambda_n,
\end{aligned}$$

where the third inequality is due to (C.7) and the sparsity condition (2.4). Then, we have

$$\begin{aligned}
\|\widehat{\beta}_{i\Delta_n} - \beta_0\|_{\max} &\leq \|\Sigma_{i\Delta_n}^{-1}\|_1 \|\Sigma_{i\Delta_n}(\widehat{\beta}_{i\Delta_n} - \beta_0)\|_{\max} \\
&\leq C\lambda_n,
\end{aligned}$$

where the last inequality is due to Assumption 1(b).

Now, we consider the  $\ell_1$  norm error bound. Let  $a_n = \|\widehat{\beta}_{i\Delta_n} - \beta_0\|_{\max}$ . Define

$$\begin{aligned}
A &= \widehat{\beta}_{i\Delta_n} - \beta_0, \\
A_1 &= \left( \widehat{\beta}_{ji\Delta_n} 1(|\widehat{\beta}_{ji\Delta_n}| \geq 2a_n); 1 \leq j \leq p \right)^\top - \beta_0.
\end{aligned}$$

Then, we have

$$\|\beta_0\|_1 - \|A_1\|_1 + \|A - A_1\|_1 \leq \|A_1 + \beta_0\|_1 + \|A - A_1\|_1 = \|\widehat{\beta}_{i\Delta_n}\|_1 \leq \|\beta_0\|_1,$$

which implies

$$\|A\|_1 \leq \|A - A_1\|_1 + \|A_1\|_1 \leq 2\|A_1\|_1.$$

Therefore, it is enough to investigate the convergence rate of  $\|A_1\|_1$ . We have

$$\begin{aligned}
\|A_1\|_1 &= \sum_{j=1}^p |\widehat{\beta}_{ji\Delta_n} 1(|\widehat{\beta}_{ji\Delta_n}| \geq 2a_n) - \beta_{j0}| \\
&\leq \sum_{j=1}^p |\widehat{\beta}_{ji\Delta_n} 1(|\widehat{\beta}_{ji\Delta_n}| \geq 2a_n) - \beta_{j0} 1(|\beta_{j0}| \geq 2a_n)| + \sum_{j=1}^p |\beta_{j0}| 1(|\beta_{j0}| \leq 2a_n) \\
&\leq \sum_{j=1}^p |\widehat{\beta}_{ji\Delta_n} 1(|\widehat{\beta}_{ji\Delta_n}| \geq 2a_n) - \beta_{j0} 1(|\beta_{j0}| \geq 2a_n)| + C s_p a_n^{1-\delta} \\
&\leq a_n \sum_{j=1}^p 1(|\widehat{\beta}_{ji\Delta_n}| \geq 2a_n) + \sum_{j=1}^p |\beta_{j0}| |1(|\beta_{j0}| \geq 2a_n) - 1(|\widehat{\beta}_{ji\Delta_n}| \geq 2a_n)| + C s_p a_n^{1-\delta} \\
&\leq a_n \sum_{j=1}^p 1(|\beta_{j0}| \geq a_n) + \sum_{j=1}^p |\beta_{j0}| |1(|\beta_{j0}| \geq 2a_n) - 1(|\widehat{\beta}_{ji\Delta_n}| \geq 2a_n)| + C s_p a_n^{1-\delta} \\
&\leq \sum_{j=1}^p |\beta_{j0}| |1(|\beta_{j0}| \geq 2a_n) - 1(|\widehat{\beta}_{ji\Delta_n}| \geq 2a_n)| + C s_p a_n^{1-\delta} \\
&\leq \sum_{j=1}^p |\beta_{j0}| 1(|\beta_{j0}| - 2a_n \leq |\beta_{j0}| - |\widehat{\beta}_{ji\Delta_n}|) + C s_p a_n^{1-\delta} \\
&\leq \sum_{j=1}^p |\beta_{j0}| 1(|\beta_{j0}| \leq 3a_n) + C s_p a_n^{1-\delta} \\
&\leq C s_p a_n^{1-\delta}.
\end{aligned} \tag{C.8}$$

■

## Proof of Theorem 2.

We denote the inverse matrix of the true instantaneous volatility matrix at time  $i\Delta_n$  by  $\Omega_0$ . By (C.6), we have, with probability greater than  $1 - p^{-1-a}$ ,

$$\begin{aligned}
\left\| \frac{1}{k_n \Delta_n} \mathcal{X}_i^\top \mathcal{X}_i \Omega_0 - \mathbf{I} \right\|_{\max} &= \left\| \left( \frac{1}{k_n \Delta_n} \mathcal{X}_i^\top \mathcal{X}_i - \frac{d}{dt} [\mathbf{X}, \mathbf{X}]_{i\Delta_n} \right) \Omega_0 \right\|_{\max} \\
&\leq \|\Omega_0\|_1 \left\| \left( \frac{1}{k_n \Delta_n} \mathcal{X}_i^\top \mathcal{X}_i - \frac{d}{dt} [\mathbf{X}, \mathbf{X}]_{i\Delta_n} \right) \right\|_{\max} \\
&\leq C(\sqrt{k_n \Delta_n} + \sqrt{\log p / k_n}).
\end{aligned}$$

Thus, by the constraint in (3.4), we have

$$P\left(\left\|\widehat{\boldsymbol{\Omega}}_{i\Delta_n}\right\|_1 \leq C\right) \geq 1 - p^{-1-a}. \quad (\text{C.9})$$

Then, similar to the proofs of Theorem 1, we can show that the statement holds. ■

## C.2 Proof of Theorem 3

**Proof of Theorem 3.** Consider (3.9) and (3.10). Without loss of generality, it is enough to show (3.9) and (3.10) for fixed  $i$ . We have

$$\begin{aligned} \widetilde{\boldsymbol{\beta}}_{i\Delta_n} - \boldsymbol{\beta}_{0,i\Delta_n} &= \frac{1}{k_n\Delta_n} \boldsymbol{\Omega}_{0,i\Delta_n} \mathcal{X}_i^\top \mathcal{Z}_i + \frac{1}{k_n\Delta_n} \widehat{\boldsymbol{\Omega}}_{i\Delta_n}^\top \mathcal{X}_i^\top \widetilde{\mathcal{X}}_i \\ &\quad - \left( \frac{1}{k_n\Delta_n} \widehat{\boldsymbol{\Omega}}_{i\Delta_n}^\top \mathcal{X}_i^\top \mathcal{X}_i - \mathbf{I} \right) (\widehat{\boldsymbol{\beta}}_{i\Delta_n} - \boldsymbol{\beta}_{0,i\Delta_n}) + \frac{1}{k_n\Delta_n} (\widehat{\boldsymbol{\Omega}}_{i\Delta_n}^\top - \boldsymbol{\Omega}_{0,i\Delta_n}) \mathcal{X}_i^\top \mathcal{Z}_i. \end{aligned} \quad (\text{C.10})$$

For  $\frac{1}{k_n\Delta_n} \widehat{\boldsymbol{\Omega}}_{i\Delta_n}^\top \mathcal{X}_i^\top \widetilde{\mathcal{X}}_i$ , by the proofs of (C.5), we have

$$\frac{1}{k_n\Delta_n} \boldsymbol{\Omega}_{0,i\Delta_n} \mathcal{X}_i^\top \widetilde{\mathcal{X}}_i = \frac{1}{k_n\Delta_n} \boldsymbol{\Omega}_{0,i\Delta_n} \mathcal{A}_i + R_{X,i},$$

where  $\|R_{X,i}\|_{\max} \leq C s_p (\log p)^{3/2} \sqrt{\Delta_n}$  with probability greater than  $1 - Cp^{-1-a}$ , and

$$\mathcal{A}_i = \left( \sum_{m=1}^p \int_{i\Delta_n}^{(i+k_n)\Delta_n} \int_{i\Delta_n}^t \sqrt{\Sigma_{\beta,mms}} dW_{ms}^* \Sigma_{jmt} dt \right)_{j=1,\dots,p}. \quad (\text{C.11})$$

By Theorem 2 and (C.5), we have, with probability greater than  $1 - Cp^{-1-a}$ ,

$$\left\| \frac{1}{k_n\Delta_n} \left( \boldsymbol{\Omega}_{0,i\Delta_n} - \widehat{\boldsymbol{\Omega}}_{i\Delta_n}^\top \right) \mathcal{X}_i^\top \widetilde{\mathcal{X}}_i \right\|_{\max} \leq C s_{\omega,p} s_p \left( \sqrt{\log p / n^{1/2}} \right)^{2-q}.$$



Thus, we have, with probability greater than  $1 - Cp^{-1-a}$ ,

$$\frac{1}{k_n \Delta_n} \widehat{\boldsymbol{\Omega}}_{i\Delta_n}^\top \mathcal{X}_i^\top \tilde{\mathcal{X}}_i = \frac{1}{k_n \Delta_n} \boldsymbol{\Omega}_{0,i\Delta_n} \mathcal{A}_i + R'_{X,i}, \quad (\text{C.12})$$

where  $\|R'_{X,i}\|_{\max} \leq C \left\{ s_{\omega,p} s_p \left( \sqrt{\log p / n^{1/2}} \right)^{2-q} + s_p (\log p)^{3/2} \sqrt{\Delta_n} \right\}$ .

For  $\left( \frac{1}{k_n \Delta_n} \widehat{\boldsymbol{\Omega}}_{i\Delta_n}^\top \mathcal{X}_i^\top \mathcal{X}_i - \mathbf{I} \right) (\widehat{\boldsymbol{\beta}}_{i\Delta_n} - \boldsymbol{\beta}_{0,i\Delta_n})$ , we have, with probability greater than  $1 - p^{-1-a}$ ,

$$\begin{aligned} & \left\| \left( \frac{1}{k_n \Delta_n} \widehat{\boldsymbol{\Omega}}_{i\Delta_n}^\top \mathcal{X}_i^\top \mathcal{X}_i - \mathbf{I} \right) (\widehat{\boldsymbol{\beta}}_{i\Delta_n} - \boldsymbol{\beta}_{0,i\Delta_n}) \right\|_{\max} \\ & \leq \left\| \frac{1}{k_n \Delta_n} \widehat{\boldsymbol{\Omega}}_{i\Delta_n}^\top \mathcal{X}_i^\top \mathcal{X}_i - \mathbf{I} \right\|_{\max} \|\widehat{\boldsymbol{\beta}}_{i\Delta_n} - \boldsymbol{\beta}_{0,i\Delta_n}\|_1 \\ & \leq C \tau_n s_p \lambda_n^{1-\delta} \\ & \leq C s_p^{2-\delta} (\log p)^{1-\delta/2} \left( \sqrt{k_n \Delta_n} + k_n^{-1/2} \right)^{2-\delta}, \end{aligned} \quad (\text{C.13})$$

where the second inequality is by Theorem 1 and (3.4). For the last term, we have

$$\begin{aligned} \left\| \frac{1}{k_n \Delta_n} (\widehat{\boldsymbol{\Omega}}_{i\Delta_n}^\top - \boldsymbol{\Omega}_{0,i\Delta_n}^\top) \mathcal{X}_i^\top \mathcal{Z}_i \right\|_{\max} & \leq \|\widehat{\boldsymbol{\Omega}}_{i\Delta_n}^\top - \boldsymbol{\Omega}_{0,i\Delta_n}^\top\|_{\infty} \left\| \frac{1}{k_n \Delta_n} \mathcal{X}_i^\top \mathcal{Z}_i \right\|_{\max} \\ & \leq C s_{\omega,p} \tau_n^{1-q} \sqrt{\log p / k_n} \\ & \leq C s_{\omega,p} (\log p)^{1-q/2} (\sqrt{k_n \Delta_n} + k_n^{-1/2})^{1-q} k_n^{-1/2}, \end{aligned} \quad (\text{C.14})$$

where the second inequality is due to Theorem 2 and (C.2), with probability greater than  $1 - Cp^{-1-a}$ . By (C.12), (C.13), and (C.14), we have, with probability greater than  $1 - p^{-a}$ ,

$$\tilde{\boldsymbol{\beta}}_{i\Delta_n} - \boldsymbol{\beta}_{0,i\Delta_n} = \frac{1}{k_n \Delta_n} \boldsymbol{\Omega}_{0,i\Delta_n} (\mathcal{X}_i^\top \mathcal{Z}_i + \mathcal{A}_i) + R_i, \quad (\text{C.15})$$

where

$$\|R_i\|_{\max} \leq C \left\{ s_p^{2-\delta} (\log p / n^{1/2})^{(2-\delta)/2} + s_p s_{\omega,p} (\log p / n^{1/2})^{(2-q)/2} + s_p (\log p)^{3/2} / n^{1/2} \right\}.$$

Consider (3.11). We have

$$\begin{aligned}\widehat{I\beta} - I\beta_0 &= k_n \Delta_n \sum_{i=0}^{\lfloor 1/(k_n \Delta_n) \rfloor - 1} \left( \tilde{\beta}_{ik_n \Delta_n} - \beta_{0,ik_n \Delta_n} \right) \\ &\quad + \sum_{i=0}^{\lfloor 1/(k_n \Delta_n) \rfloor - 1} \int_{ik_n \Delta_n}^{(i+1)k_n \Delta_n} (\beta_{0,ik_n \Delta_n} - \beta_{0,t}) dt - \int_{\lfloor 1/(k_n \Delta_n) \rfloor k_n \Delta_n}^1 \beta_{0,t} dt.\end{aligned}$$

First, we consider the discretization error terms. Since the coefficient process has the sub-Gaussian tail, we can show, with probability greater than  $1 - p^{-1-a}$ ,

$$\left\| \sum_{i=0}^{\lfloor 1/(k_n \Delta_n) \rfloor - 1} \int_{ik_n \Delta_n}^{(i+1)k_n \Delta_n} (\beta_{0,ik_n \Delta_n} - \beta_{0,t}) dt \right\|_{\max} \leq C \sqrt{\log p/n}.$$

Also, by Assumption 1(b), we have

$$\left\| \int_{\lfloor 1/(k_n \Delta_n) \rfloor k_n \Delta_n}^1 \beta_{0,t} dt \right\|_{\max} \leq C n^{-1/2} \text{ a.s.}$$

Consider  $\sum_{i=0}^{\lfloor 1/(k_n \Delta_n) \rfloor - 1} \left( \tilde{\beta}_{ik_n \Delta_n} - \beta_{0,ik_n \Delta_n} \right)$ . By (3.9), we have

$$\sum_{i=0}^{\lfloor 1/(k_n \Delta_n) \rfloor - 1} \left( \tilde{\beta}_{ik_n \Delta_n} - \beta_{0,ik_n \Delta_n} \right) = \sum_{i=0}^{\lfloor 1/(k_n \Delta_n) \rfloor - 1} \frac{1}{k_n \Delta_n} \mathbf{\Omega}_{0,ik_n \Delta_n} (\mathcal{X}_{ik_n}^\top \mathcal{Z}_{ik_n} + \mathcal{A}_{ik_n}) + R_{ik_n},$$

and, similar to the proofs of (C.15), we can show, with probability greater than  $1 - p^{-1-a}$ ,

$$\begin{aligned}\left\| \sum_{i=0}^{\lfloor 1/(k_n \Delta_n) \rfloor - 1} R_{ik_n} \right\|_{\max} &\leq \sum_{i=0}^{\lfloor 1/(k_n \Delta_n) \rfloor - 1} \|R_{ik_n}\|_{\max} \\ &\leq C \frac{1}{k_n \Delta_n} \left\{ s_p^{2-\delta} (\log p/n^{1/2})^{(2-\delta)/2} + s_p s_{\omega,p} (\log p/n^{1/2})^{(2-q)/2} + s_p (\log p)^{3/2}/n^{1/2} \right\}.\end{aligned}$$

Since the inverse matrix process  $\mathbf{\Omega}_{0,ik_n \Delta_n}$  is bounded and  $\mathcal{X}$  and  $\mathcal{Z}$  have sub-Gaussian tails, similar to the proofs of Theorem 1 (Kim and Wang, 2016), we can show, with probability

greater than  $1 - p^{-1-a}$ ,

$$\left\| \sum_{i=0}^{[1/(k_n \Delta_n)]-1} \Omega_{0,ik_n \Delta_n} \mathcal{X}_{ik_n}^\top \mathcal{Z}_{ik_n} \right\|_{\max} \leq C \sqrt{\log p/n}.$$

Finally, we consider  $\Omega_{0,ik_n \Delta_n} \mathcal{A}_{ik_n}$  terms. Note that  $\mathcal{A}_{ik_n}$ 's are martingales with sub-Gaussian tails. Thus, by Azuma-Hoeffding inequality, we have, with probability greater than  $1 - p^{-1-a}$ ,

$$\left\| \sum_{i=0}^{[1/(k_n \Delta_n)]-1} \Omega_{0,ik_n \Delta_n} \mathcal{A}_{ik_n} \right\|_{\max} \leq C s_p \sqrt{\log p n}^{-1/2}.$$

Therefore, the statement (3.11) is shown. ■

### C.3 Proof of Theorem 4

**Proof of Theorem 4.** By (3.11), we can find  $h_n$  such that, with probability greater than  $1 - p^{-a}$ ,

$$\|\widehat{I\beta} - I\beta_0\|_{\max} \leq h_n/2. \quad (\text{C.16})$$

We show that the statement holds under the event (C.16). Similar to the proof of (C.8), we can show

$$\|\widetilde{I\beta} - I\beta_0\|_1 \leq C s_p h_n^{1-\delta}.$$

■

## C.4 Proof of Theorem 5

**Proof of Theorem 5.** Define

$$\mathcal{Y}_i^c = \begin{pmatrix} \Delta_{i+1}^n Y^c \\ \Delta_{i+2}^n Y^c \\ \vdots \\ \Delta_{i+k_n}^n Y^c \end{pmatrix} \quad \text{and} \quad \mathcal{X}_i^c = \begin{pmatrix} \Delta_{i+1}^n \mathbf{X}^{c\top} \\ \Delta_{i+2}^n \mathbf{X}^{c\top} \\ \vdots \\ \Delta_{i+k_n}^n \mathbf{X}^{c\top} \end{pmatrix}.$$

For some large constant  $C > 0$ , let

$$E_1 = \left\{ \max_{i,j} |\Delta_i^n X_j^c| \leq C \sqrt{\log pn}^{-1/2} \right\} \cap \left\{ \max_{i,j} |\Delta_i^n Y_j^c| \leq C s_p \sqrt{\log pn}^{-1/2} \right\},$$

$$E_2 = \left\{ \max_{i,j} \sum_{k=1}^{k_n} \mathbf{1}_{\{|\Delta_{i+k}^n X_j^c| > v_{j,n}\}} \leq C \log p \right\} \cap \left\{ \max_{i,j} \int_{i\Delta_n}^{(i+k_n)\Delta_n} d\Lambda_{jt} \leq C \log p \right\}.$$

By the boundedness condition Assumption 1(b) and sparsity condition (2.4), we can show

$$P(E_1) \geq 1 - p^{-2-a}.$$

Under the event  $E_1$ , we have, for large  $n$ ,

$$\max_{i,j} \sum_{k=1}^{k_n} \mathbf{1}_{\{|\Delta_{i+k}^n X_j^c| > v_{j,n}\}} \leq \max_{i,j} \int_{i\Delta_n}^{(i+k_n)\Delta_n} d\Lambda_{jt},$$

where  $\int_{i\Delta_n}^{(i+k_n)\Delta_n} d\Lambda_{jt}$  is a Poisson with the intensity  $Ck_n\Delta_n$  for some constant  $C > 0$ , and

$$P\left(\max_{i,j} \int_{i\Delta_n}^{(i+k_n)\Delta_n} d\Lambda_{jt} \geq C \log p\right) \leq p^{-2-a}.$$

Thus, we have

$$P(E_1 \cap E_2) \geq 1 - p^{-1-a}. \tag{C.17}$$

We have

$$\begin{aligned}
& \sum_{k=1}^{k_n} \Delta_{i+k}^n X_j \mathbf{1}_{\{|\Delta_{i+k}^n X_j| \leq v_{j,n}\}} \Delta_{i+k}^n X_l \mathbf{1}_{\{|\Delta_{i+k}^n X_l| \leq v_{l,n}\}} - \Delta_{i+k}^n X_j^c \Delta_{i+k}^n X_l^c \\
&= \sum_{k=1}^{k_n} \Delta_{i+k}^n X_j^c \Delta_{i+k}^n X_l^c (\mathbf{1}_{\{|\Delta_{i+k}^n X_j| \leq v_{j,n}\}} \mathbf{1}_{\{|\Delta_{i+k}^n X_l| \leq v_{l,n}\}} - 1) \\
&\quad + \sum_{k=1}^{k_n} (\Delta_{i+k}^n X_j^c \Delta_{i+k}^n X_l^J + \Delta_{i+k}^n X_j^J \Delta_{i+k}^n X_l^c + \Delta_{i+k}^n X_j^J \Delta_{i+k}^n X_l^J) \mathbf{1}_{\{|\Delta_{i+k}^n X_j| \leq v_{j,n}\}} \mathbf{1}_{\{|\Delta_{i+k}^n X_l| \leq v_{l,n}\}} \\
&= (I)_{ijl} + (II)_{ijl}.
\end{aligned}$$

Under the event  $E_1 \cap E_2$ , we have

$$\begin{aligned}
\max_{i,j,l} |(I)_{ijl}| &\leq C \max_{i,j} |\Delta_i^n X_j^c|^2 \times \max_{i,j} \sum_{k=1}^{k_n} \mathbf{1}_{\{|\Delta_{i+k}^n X_j| > v_{j,n}\}} \\
&\leq C(\log p)^2/n
\end{aligned}$$

and

$$\begin{aligned}
\max_{i,j,l} |(II)_{ijl}| &\leq C \sqrt{\log pn}^{-\rho} \max_{i,j} |\Delta_i^n X_j^c| \times \max_{i,j} \int_{i\Delta_n}^{(i+k_n)\Delta_n} d\Lambda_{jt} \\
&\quad + C \left( \sqrt{\log pn}^{-\rho} \right)^2 \max_{i,j} \int_{i\Delta_n}^{(i+k_n)\Delta_n} d\Lambda_{jt} \\
&\leq C(\log p)^2 n^{-2\varrho}.
\end{aligned}$$

Thus, by (C.17), we have, with probability greater than  $1 - p^{-1-a}$ ,

$$\begin{aligned}
\max_i \frac{1}{k_n \Delta_n} \left\| \widehat{\mathcal{X}}_i^{c\top} \widehat{\mathcal{X}}_i^c - \mathcal{X}_i^{c\top} \mathcal{X}_i^c \right\|_{\max} &\leq C(\log p)^2 n^{1/2-2\varrho} \\
&\leq C \sqrt{\log pn}^{-1/4},
\end{aligned} \tag{C.18}$$

and similarly, we can show, with probability greater than  $1 - p^{-1-a}$ ,

$$\max_i \frac{1}{k_n \Delta_n} \left\| \widehat{\mathcal{X}}_i^{c\top} \widehat{\mathcal{Y}}_i^c - \mathcal{X}_i^{c\top} \mathcal{Y}_i^c \right\|_{\max} \leq C s_p (\log p)^2 n^{1/2-2\varrho}$$

$$\leq C s_p \sqrt{\log p n}^{-1/4}. \quad (\text{C.19})$$

Consider  $\left\| \sum_{i=0}^{\lceil 1/(k_n \Delta_n) \rceil - 1} \hat{\Omega}_{ik_n \Delta_n}^\top \left[ \hat{\mathcal{X}}_{ik_n}^{c\top} (\hat{\mathcal{Y}}_{ik_n}^c - \hat{\mathcal{X}}_{ik_n}^c \hat{\beta}_{ik_n \Delta_n}) - \mathcal{X}_{ik_n}^{c\top} (\mathcal{Y}_{ik_n}^c - \mathcal{X}_{ik_n}^c \hat{\beta}_{ik_n \Delta_n}) \right] \right\|_\infty$ . By (3.7), (3.8), and (C.9), we have, with probability at least  $1 - 2p^{-1-a}$ ,

$$\begin{aligned} & \left\| \sum_{i=0}^{\lceil 1/(k_n \Delta_n) \rceil - 1} \hat{\Omega}_{ik_n \Delta_n}^\top \left[ \hat{\mathcal{X}}_{ik_n}^{c\top} (\hat{\mathcal{Y}}_{ik_n}^c - \hat{\mathcal{X}}_{ik_n}^c \hat{\beta}_{ik_n \Delta_n}) - \mathcal{X}_{ik_n}^{c\top} (\mathcal{Y}_{ik_n}^c - \mathcal{X}_{ik_n}^c \hat{\beta}_{ik_n \Delta_n}) \right] \right\|_\infty \\ & \leq \left\| \sum_{i=0}^{\lceil 1/(k_n \Delta_n) \rceil - 1} \Omega_{0,ik_n \Delta_n} \left[ \hat{\mathcal{X}}_{ik_n}^{c\top} (\hat{\mathcal{Y}}_{ik_n}^c - \hat{\mathcal{X}}_{ik_n}^c \beta_{0,ik_n \Delta_n}) - \mathcal{X}_{ik_n}^{c\top} (\mathcal{Y}_{ik_n}^c - \mathcal{X}_{ik_n}^c \beta_{0,ik_n \Delta_n}) \right] \right\|_\infty \\ & \quad + \left\| \sum_{i=0}^{\lceil 1/(k_n \Delta_n) \rceil - 1} \left\| \hat{\Omega}_{ik_n \Delta_n} - \Omega_{0,ik_n \Delta_n} \right\|_1 \times \left\| \hat{\mathcal{X}}_{ik_n}^{c\top} \hat{\mathcal{Y}}_{ik_n}^c - \mathcal{X}_{ik_n}^{c\top} \mathcal{Y}_{ik_n}^c \right\|_{\max} \right\|_\infty \\ & \quad + \left\| \sum_{i=0}^{\lceil 1/(k_n \Delta_n) \rceil - 1} \left\| \hat{\Omega}_{ik_n \Delta_n} \right\|_1 \times \left\| \hat{\mathcal{X}}_{ik_n}^{c\top} \hat{\mathcal{X}}_{ik_n}^c - \mathcal{X}_{ik_n}^{c\top} \mathcal{X}_{ik_n}^c \right\|_{\max} \times \left\| \hat{\beta}_{ik_n \Delta_n} - \beta_{0,ik_n \Delta_n} \right\|_1 \right\|_\infty \\ & \quad + \left\| \sum_{i=0}^{\lceil 1/(k_n \Delta_n) \rceil - 1} \left\| \hat{\Omega}_{ik_n \Delta_n} - \Omega_{0,ik_n \Delta_n} \right\|_1 \times \left\| \hat{\mathcal{X}}_{ik_n}^{c\top} \hat{\mathcal{X}}_{ik_n}^c - \mathcal{X}_{ik_n}^{c\top} \mathcal{X}_{ik_n}^c \right\|_{\max} \times \left\| \beta_{0,ik_n \Delta_n} \right\|_1 \right\|_\infty \\ & \leq \left\| \sum_{i=0}^{\lceil 1/(k_n \Delta_n) \rceil - 1} \Omega_{0,ik_n \Delta_n} \left[ \hat{\mathcal{X}}_{ik_n}^{c\top} (\hat{\mathcal{Y}}_{ik_n}^c - \hat{\mathcal{X}}_{ik_n}^c \beta_{0,ik_n \Delta_n}) - \mathcal{X}_{ik_n}^{c\top} (\mathcal{Y}_{ik_n}^c - \mathcal{X}_{ik_n}^c \beta_{0,ik_n \Delta_n}) \right] \right\|_\infty \\ & \quad + C \left\{ s_p^{2-\delta} (\log p / n^{1/2})^{(2-\delta)/2} + s_p s_{\omega,p} (\log p / n^{1/2})^{(2-q)/2} \right\}. \end{aligned} \quad (\text{C.20})$$

For the first term, let  $\mathbf{u}_t = (u_{1,t}, \dots, u_{p,t})^\top$  be any  $p$ -dimensional process, which is independent of  $\Lambda_t$  and satisfies  $\|\mathbf{u}_t\|_1 \leq C$ . By the Jensen's inequality, we have

$$\begin{aligned} & \mathbb{E} \left[ \exp \left( \mathbf{u}_{ik_n \Delta_n}^\top \int_{ik_n \Delta_n}^{(i+1)k_n \Delta_n} d\Lambda_t \right) \middle| \mathcal{F}_{ik_n \Delta_n} \right] \\ & \leq \sum_{j=1}^p \frac{|u_{j,ik_n \Delta_n}|}{\|\mathbf{u}_{ik_n \Delta_n}\|_1} \mathbb{E} \left[ \exp \left( \|\mathbf{u}_{ik_n \Delta_n}\|_1 \int_{ik_n \Delta_n}^{(i+1)k_n \Delta_n} d\Lambda_{jt} \right) \middle| \mathcal{F}_{ik_n \Delta_n} \right] \\ & \leq \exp(C n^{-1/2}), \end{aligned}$$

where the last inequality is from the moment generating function of the Poisson distribution. Then, by the Markov inequality, we have

$$\begin{aligned}
& P \left( \sum_{i=0}^{\lfloor 1/(k_n \Delta_n) \rfloor - 1} \mathbf{u}_{ik_n \Delta_n}^\top \int_{ik_n \Delta_n}^{(i+1)k_n \Delta_n} d\mathbf{\Lambda}_t \geq (a+3) \log p \right) \\
& \leq p^{-3-a} \mathbb{E} \left[ \prod_{i=0}^{\lfloor 1/(k_n \Delta_n) \rfloor - 1} \exp \left( \mathbf{u}_{ik_n \Delta_n}^\top \int_{ik_n \Delta_n}^{(i+1)k_n \Delta_n} d\mathbf{\Lambda}_t \right) \right] \\
& \leq Cp^{-3-a}.
\end{aligned} \tag{C.21}$$

Note that  $\beta_t/s_p$  and  $\mathbf{\Omega}_t$  are bounded. Hence, similar to the proofs of (C.18), we can show, with probability at least  $1 - p^{-1-a}$ ,

$$\left\| \sum_{i=0}^{\lfloor 1/(k_n \Delta_n) \rfloor - 1} \mathbf{\Omega}_{0,ik_n \Delta_n} \left[ \hat{\mathcal{X}}_{ik_n}^{c\top} \hat{\mathcal{X}}_{ik_n}^c - \mathcal{X}_{ik_n}^{c\top} \mathcal{X}_{ik_n}^c \right] \beta_{0,ik_n \Delta_n} \right\|_\infty \leq Cs_p n^{-3/4} \sqrt{\log p}, \tag{C.22}$$

and similarly, we can show, with probability at least  $1 - p^{-1-a}$ ,

$$\left\| \sum_{i=0}^{\lfloor 1/(k_n \Delta_n) \rfloor - 1} \mathbf{\Omega}_{0,ik_n \Delta_n} \left[ \hat{\mathcal{X}}_{ik_n}^{c\top} \hat{\mathcal{Y}}_{ik_n}^c - \mathcal{X}_{ik_n}^{c\top} \mathcal{Y}_{ik_n}^c \right] \right\|_\infty \leq Cs_p n^{-3/4} \sqrt{\log p}. \tag{C.23}$$

From (C.20), (C.22), and (C.23), we have, with probability at least  $1 - 4p^{-1-a}$ ,

$$\begin{aligned}
& \left\| \sum_{i=0}^{\lfloor 1/(k_n \Delta_n) \rfloor - 1} \hat{\mathbf{\Omega}}_{ik_n \Delta_n}^\top \left[ \hat{\mathcal{X}}_{ik_n}^{c\top} (\hat{\mathcal{Y}}_{ik_n}^c - \hat{\mathcal{X}}_{ik_n}^c \hat{\beta}_{ik_n \Delta_n}) - \mathcal{X}_{ik_n}^{c\top} (\mathcal{Y}_{ik_n}^c - \mathcal{X}_{ik_n}^c \hat{\beta}_{ik_n \Delta_n}) \right] \right\|_\infty \\
& \leq C \left\{ s_p^{2-\delta} (\log p / n^{1/2})^{(2-\delta)/2} + s_p s_{\omega,p} (\log p / n^{1/2})^{(2-q)/2} \right\}.
\end{aligned} \tag{C.24}$$

By (C.18), (C.19), and (C.24), the effect of jumps is negligible. Thus, the statement can be shown by Theorem 4. ■

## D A simulation setup

We generated the data with frequency  $1/n^{all}$  and considered the following time series regression jump diffusion model:

$$\begin{aligned} dY_t &= \boldsymbol{\beta}_t^\top d\mathbf{X}_t^c + dZ_t + J_t^y d\Lambda_t^y, \\ d\mathbf{X}_t &= d\mathbf{X}_t^c + d\mathbf{X}_t^J, \quad d\mathbf{X}_t^c = \boldsymbol{\sigma}_t d\mathbf{B}_t, \quad d\mathbf{X}_t^J = \mathbf{J}_t d\boldsymbol{\Lambda}_t, \quad dZ_t = \nu_t dW_t, \end{aligned}$$

where  $\mathbf{B}_t$  and  $W_t$  are  $p$ -dimensional and one-dimensional independent Brownian motions, respectively,  $\mathbf{J}_t = (J_{1t}, \dots, J_{pt})^\top$  and  $J_t^y$  are jump sizes, and  $\boldsymbol{\Lambda}_t = (\Lambda_{1t}, \dots, \Lambda_{pt})^\top$  and  $\Lambda_t^y$  are the Poisson processes with the intensities  $(10, \dots, 10)^\top$  and 5, respectively. The jump sizes  $J_{it}$  and  $J_t^y$  were independently generated from the Gaussian distribution with a mean of 0 and standard deviation of 0.05. We set the initial values  $X_{i0}$  and  $Y_0$  to 0, while  $\nu_t$  follows the OU process

$$d\nu_t = 2(0.12 - \nu_t)dt + 0.03d\mathbf{W}_t^\nu,$$

where  $\nu_0 = 0.15$  and  $\mathbf{W}_t^\nu$  is one-dimensional independent Brownian motion. The instantaneous volatility process  $\boldsymbol{\sigma}_t$  was taken to be a Cholesky decomposition of  $\boldsymbol{\Sigma}_t = (\Sigma_{ijt})_{1 \leq i, j \leq p}$ , where  $\Sigma_{ijt} = \xi_t 0.7^{|i-j|}$  and  $\xi_t$  satisfies

$$d\xi_t = 6(0.3 - \xi_t)dt + 0.12d\mathbf{W}_t^\xi,$$

where  $\xi_0 = 0.5$  and  $\mathbf{W}_t^\xi$  is one-dimensional independent Brownian motion. For the coefficient process  $\boldsymbol{\beta}_t$ , we considered the time-varying coefficient and constant coefficient processes, where  $[s_p]$  factors are only significant. We first generated the time-varying coefficient process as follows:

$$d\boldsymbol{\beta}_t = \boldsymbol{\mu}_{\boldsymbol{\beta},t}dt + \boldsymbol{\nu}_{\boldsymbol{\beta},t}d\mathbf{W}_t^\beta,$$



where  $\boldsymbol{\mu}_{\beta,t} = (\mu_{1,\beta,t}, \dots, \mu_{p,\beta,t})^\top$ ,  $\boldsymbol{\nu}_{\beta,t} = (\nu_{i,j,\beta,t})_{1 \leq i,j \leq p}$ , and  $\mathbf{W}_t^\beta$  is a  $p$ -dimensional independent Brownian motion. We set the process  $(\nu_{i,j,\beta,t})_{1 \leq i,j \leq [s_p]}$  as  $\zeta_t \mathbf{I}_{[s_p]}$ , where  $\mathbf{I}_{[s_p]}$  is the  $[s_p]$ -dimensional identity matrix and  $\zeta_t$  was generated as follows:

$$d\zeta_t = 4(0.5 - \zeta_t) dt + 0.2 d\mathbf{W}_t^\zeta,$$

where  $\zeta_0 = 0.4$  and  $\mathbf{W}_t^\zeta$  is one-dimensional independent Brownian motion. For  $i = 1, \dots, [s_p]$ , we took the initial value  $\beta_{i0}$  as  $2^{3-i}$  and set  $\mu_{i,\beta,t} = 0.05$  for  $0 \leq t \leq 1$ . We set  $\beta_{it}$ ,  $i = [s_p] + 1, \dots, p$ , as zero. In contrast, for the constant coefficient process, we set  $\beta_{it} = 2^{3-i}$  for  $i = 1, \dots, [s_p]$  and  $0 \leq t \leq 1$ , while the other  $\beta_{it}$ 's were set to 0. We chose  $p = 100$ ,  $s_p = \log p$ ,  $n^{all} = 4000$ , and we varied  $n$  from 1000 to 4000.

## E Visualization of TED procedure and simulated co-efficient dynamics

To check whether TED accurately captures the time-varying behavior of the true coefficients, we present trajectory plots of the true coefficients and their debiased instantaneous estimates obtained from the TED procedure. Figures 6 and 7 illustrate these coefficient dynamics for selected simulation paths under different sample sizes  $n = 1000, 2000, 4000$ , corresponding to the time-varying coefficient and constant coefficient simulations, respectively. We selected three representative simulation paths based on the 25th percentile (Q1), median (Q2), and 75th percentile (Q3) of the  $\ell_2$ -norm estimation errors of TED at the largest sample size  $n = 4000$ , as well as the average path computed across all simulation paths. We present the paths for all true nonzero coefficients and additionally include the path of the largest estimated integrated coefficient among the coefficients whose true values are zero, prior to thresholding. From Figures 6 and 7, we find that the estimated instantaneous coefficients capture the temporal dynamics more accurately as the sample size increases.

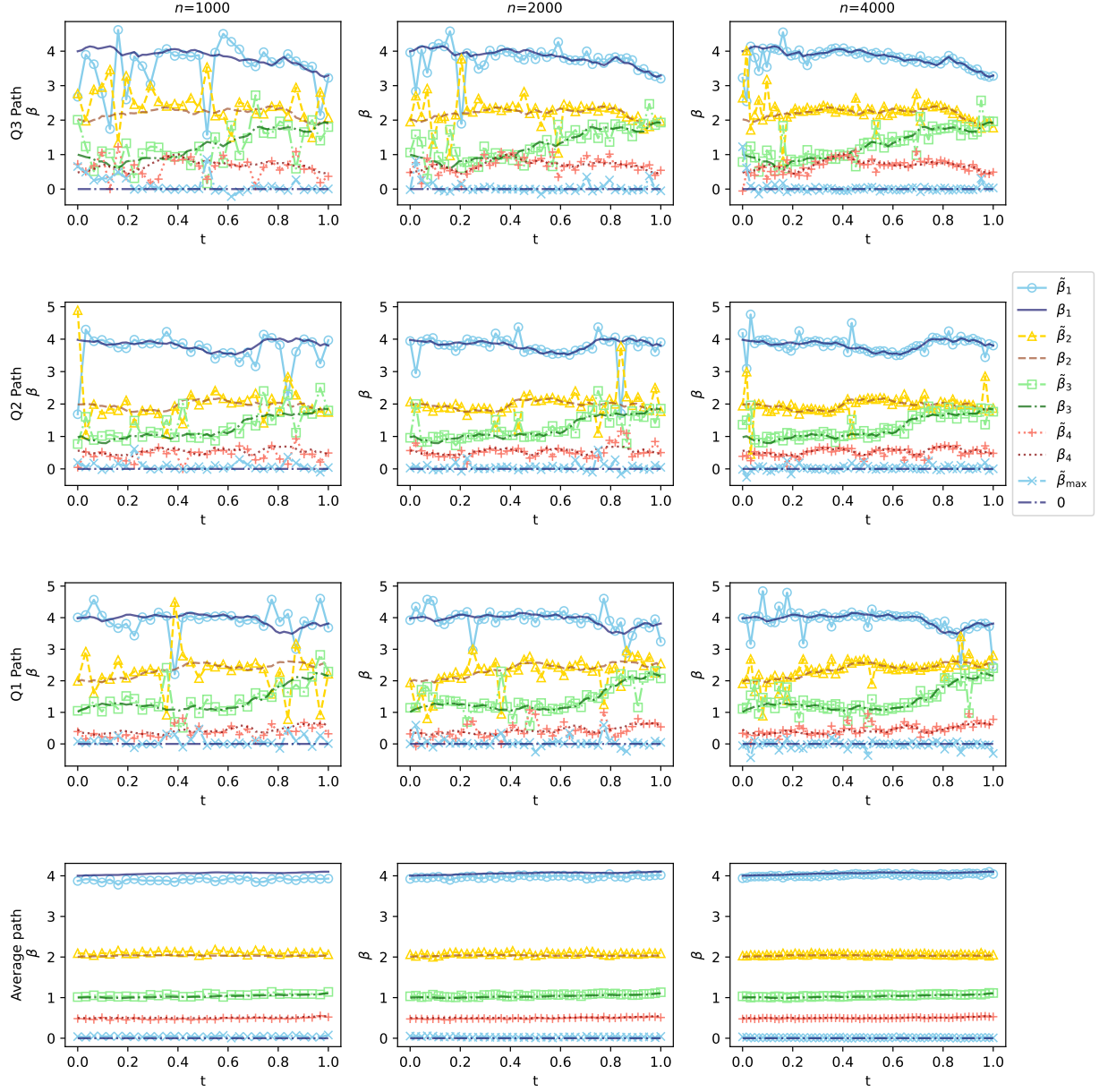


Figure 6: Trajectory plots of the true time-varying coefficients and their corresponding TED estimates under different sample sizes  $n = 1000, 2000, 4000$ . Each row represents simulation paths selected based on the 75th percentile (Q3), median (Q2), and 25th percentile (Q1) of the  $\ell_2$ -norm errors at the largest sample size  $n = 4000$ , along with the average path. All nonzero coefficients and the largest estimated integrated coefficient among true zero coefficients before thresholding are presented.

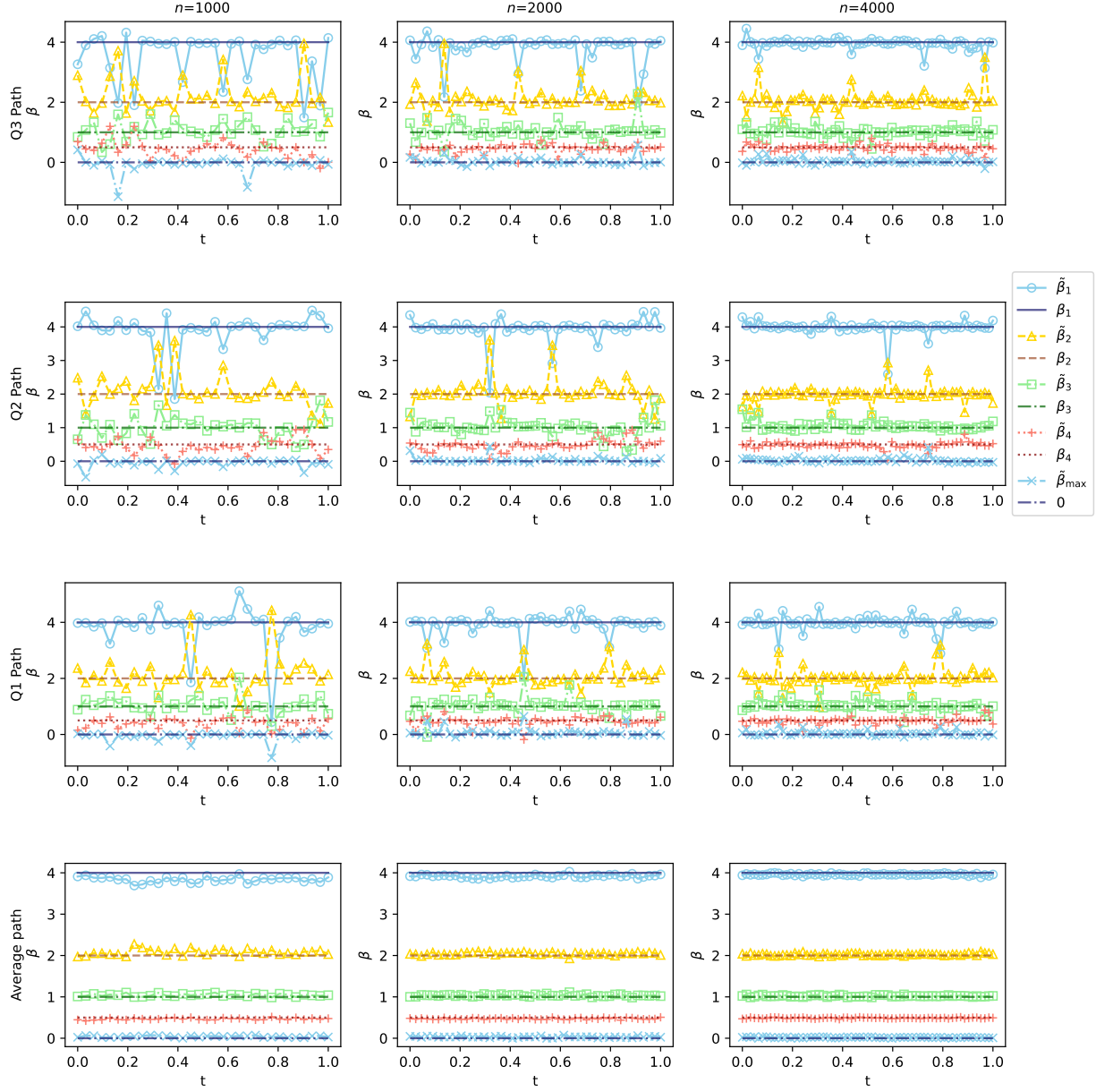


Figure 7: Trajectory plots of the true constant coefficients and their corresponding TED estimates under different sample sizes  $n = 1000, 2000, 4000$ . Each row represents simulation paths selected based on the 75th percentile (Q3), median (Q2), and 25th percentile (Q1) of the  $\ell_2$ -norm errors at the largest sample size  $n = 4000$ , along with the average path. All nonzero coefficients and the largest estimated integrated coefficient among true zero coefficients before thresholding are presented.

## F Additional empirical analyses

To investigate the impact of each tuning parameter on the performance of the TED estimator, we conducted sensitivity analyses by varying one parameter at a time while keeping the

others fixed according to the scheme discussed in Section 3.4. Figure 8 shows the sensitivity

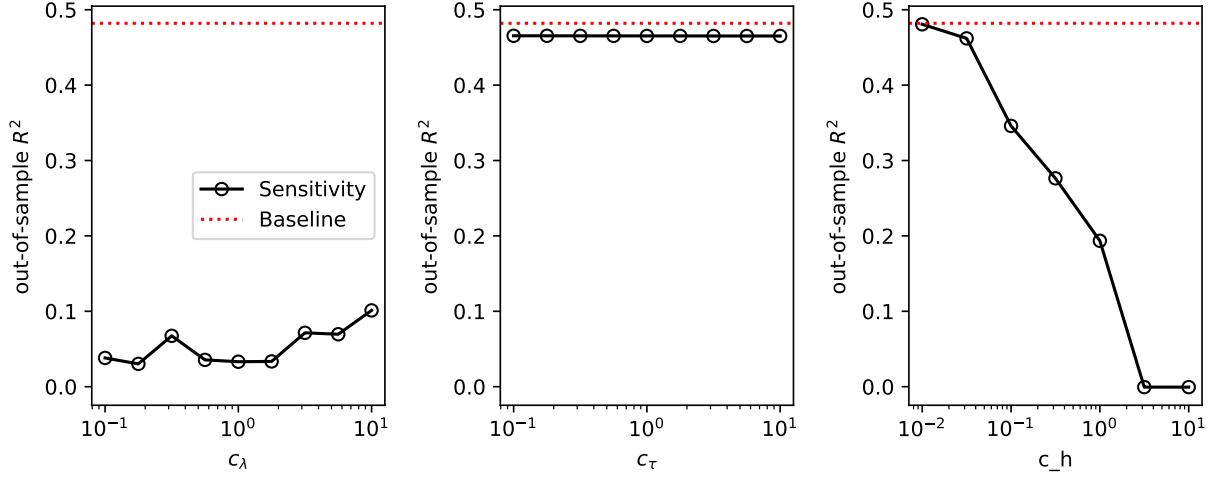


Figure 8: Sensitivity analysis of the TED estimator with respect to tuning parameters  $c_\lambda$ ,  $c_\tau$ , and  $c_h$ .

analysis results for the TED estimator with respect to the tuning parameters  $c_\lambda$ ,  $c_\tau$ , and  $c_h$ . The horizontal dashed line (baseline) indicates the result obtained by using the tuning parameter selection method described in Section 3.4. Each solid line corresponds to the results obtained by varying one tuning parameter while the others are chosen according to the baseline method. We varied  $c_\lambda$  and  $c_\tau$  from 0.1 to 10, and  $c_h$  from 0.01 to 10, using a logarithmically equidistant grid. From Figure 8, we find that selecting proper values for all three tuning parameters is crucial. Specifically, using a single fixed value for  $c_\lambda$  and  $c_\tau$  results in worse performance. This may be because of the time-varying sparsity of the coefficients and the inverse covariance matrix. On the other hand, smaller values of  $c_h$  tend to yield better performance. This may be due to the presence of weak factors that have only minor impacts on individual assets.

Our theoretical results hold for any instantaneous coefficient estimators having the same convergence rate in (3.7) and the bias term in (3.9). As part of a comprehensive analysis, we replaced the Dantzig selector with alternative methods and compared their performances against our results. Table 3 shows the annual average out-of-sample  $R^2$  of the TED frame-

Table 3: The annual average out-of-sample  $R^2$  of the TED framework using different penalized regression methods to estimate the instantaneous coefficients.

Period	RV (%)	Out-of-sample $R^2$									
		TED	ADAN	LAS	ALAS	RID	ARID	ELA	AELA	SCA	ASCA
whole	12.0	0.482	0.475	0.433	0.481	0.466	0.467	0.430	0.481	0.438	0.429
2013	7.9	0.613	0.602	0.539	0.613	0.596	0.591	0.546	0.613	0.523	0.525
2014	8.8	0.475	0.472	0.418	0.475	0.455	0.455	0.411	0.473	0.425	0.419
2015	10.2	0.505	0.496	0.473	0.504	0.485	0.488	0.475	0.504	0.475	0.460
2016	10.0	0.510	0.501	0.469	0.506	0.490	0.498	0.468	0.509	0.469	0.457
2017	5.5	0.398	0.391	0.353	0.399	0.396	0.383	0.350	0.399	0.354	0.355
2018	13.0	0.538	0.532	0.485	0.538	0.519	0.518	0.472	0.536	0.498	0.490
2019	9.1	0.461	0.454	0.407	0.460	0.446	0.444	0.398	0.462	0.420	0.412
2020	22.8	0.366	0.360	0.328	0.365	0.352	0.368	0.328	0.365	0.344	0.319

work using different penalized regression methods, such as LASSO (LAS), Ridge (RID), elastic net (ELA), and SCAD (SCA), as well as their adaptive versions including the adaptive versions of Dantzig (ADAN), LASSO (ALAS), Ridge (ARID), elastic net (AELA), and SCAD (ASCA), for estimating the instantaneous coefficients. The adaptive methods impose different weights on the penalty terms for each coefficient. Heavier penalties are assigned to smaller preliminary estimates, and lighter penalties to larger ones, where the preliminary estimates can be obtained from methods such as Ridge regression (Zou, 2006; Zou and Zhang, 2009). From Table 3, we find that ALAS and AELA show comparable performance to the original TED, although TED achieves the best average performance. This may be because those penalties address sparsity as well as the shrinkage bias. Specifically, ALAS and AELA assign different penalty weights to each coefficient, inversely proportional to the magnitude of preliminary estimates. This procedure effectively reduces bias for significant coefficients while shrinking insignificant coefficients more aggressively.

To check whether our results are sensitive to the inverse covariance estimation method, we replaced the CLIME estimator with an alternative method. If covariates have a factor structure, we can estimate the inverse instantaneous volatility matrix using the POET method (Fan et al., 2013). Specifically, we can apply the POET estimator to estimate the

covariance matrix and then obtain the arithmetic inversion of this estimate. We call this TED-POET. This method is computationally more efficient than CLIME and achieves the  $\ell_1$  convergence rate of  $O_p(s'_{\omega,p}(\sqrt{\log pn}^{-1/4} + p^{-1/2})^{1-q})$ , where  $s'_{\omega,p} = \max_{i \leq p} \sum_{j \leq p} |\sigma_{u,ij}|^q$ . Under  $n^{1/4}/\sqrt{p \log p} \rightarrow 0$  and the same sparsity levels  $s_{\omega,p}$  and  $s'_{\omega,p}$ , the convergence rate of the POET estimator is asymptotically the same as that of the CLIME estimator,  $O_p(s_{\omega,p}(\sqrt{\log p} \times n^{-1/4})^{1-q})$ . Table 4 shows the in-sample and out-of-sample  $R^2$  for TED and TED-POET.

Table 4: In-sample and out-of-sample  $R^2$  for TED and TED-POET.

Period	RV (%)	In-sample $R^2$		Out-of-sample $R^2$	
		TED	TED-POET	TED	TED-POET
whole	12.0	0.539	0.525	0.482	0.474
2013	7.9	0.667	0.675	0.613	0.620
2014	8.8	0.525	0.498	0.475	0.447
2015	10.2	0.573	0.538	0.505	0.506
2016	10.0	0.570	0.537	0.510	0.479
2017	5.5	0.453	0.447	0.398	0.398
2018	13.0	0.586	0.577	0.538	0.542
2019	9.1	0.515	0.520	0.461	0.462
2020	22.8	0.425	0.410	0.366	0.351

From Table 4, we find that TED-POET shows comparable performance to TED, although TED performs better in a few subperiods. This may be because the covariance matrix of the factor zoo does not always conform to a low-rank-plus-sparse representation across periods.

We also compared the performance of TED with the benchmarks using an alternative measure of predictive accuracy, the mean absolute error (MAE). Specifically, we measured it as the average of the absolute differences between the observed high-frequency returns of the assets and the returns predicted by the estimated coefficient using the high-frequency factors for the next month. Table 5 shows the annual average MAE for the TED, AKX, AKX6, and various regression estimators across the five assets. We find that TED generally outperforms the other methods in terms of MAE. This highlights the advantage of TED in accommodating the time-varying nature of coefficients for more accurate predictions.

Table 5: The annual average out-of-sample MAE for the TED, AKX, AKX6, and various regression estimators across the five assets.

Period	RV (%)	Out-of-sample MAE $\times 1000$														
		TED	AKX	AKX6	OLS6	LAS	ALAS	RID	ARID	ELA	AELA	SCA	ASCA	BAY	DAN	ADAN
whole	12.0	0.598	0.740	0.878	0.799	0.627	0.608	0.613	0.609	0.611	0.616	0.616	0.749	0.670	0.623	0.641
2013	7.9	0.431	0.645	0.788	0.716	0.489	0.426	0.435	0.427	0.455	0.432	0.482	0.614	0.485	0.436	0.455
2014	8.8	0.535	0.668	0.769	0.707	0.563	0.545	0.541	0.541	0.546	0.553	0.554	0.672	0.595	0.555	0.571
2015	10.2	0.542	0.701	0.856	0.757	0.570	0.546	0.562	0.555	0.555	0.554	0.559	0.677	0.624	0.563	0.580
2016	10.0	0.502	0.668	0.814	0.732	0.536	0.515	0.524	0.518	0.520	0.522	0.527	0.626	0.589	0.526	0.547
2017	5.5	0.441	0.551	0.619	0.573	0.458	0.454	0.456	0.456	0.448	0.463	0.452	0.519	0.495	0.469	0.480
2018	13.0	0.616	0.776	0.968	0.854	0.649	0.624	0.632	0.625	0.632	0.629	0.632	0.804	0.673	0.643	0.657
2019	9.1	0.524	0.649	0.763	0.692	0.548	0.534	0.541	0.535	0.536	0.542	0.535	0.655	0.588	0.543	0.566
2020	22.8	1.181	1.257	1.438	1.350	1.192	1.205	1.197	1.201	1.180	1.216	1.177	1.411	1.294	1.232	1.254

We analyzed how TED performance changes with different sampling frequencies—10-min and 30-min log price data—compared to our baseline frequency (5-min). We note that sampling frequencies higher than 5-min are inappropriate due to microstructure noise (Aït-Sahalia and Xiu, 2019a). Tables 6 and 7 report the annual average out-of-sample  $R^2$  results

Table 6: The annual average in-sample and out-of-sample  $R^2$  for the TED, AKX, AKX6, and various regression estimators across the five assets using 10-min sampling frequency data.

Period	RV (%)	In-sample $R^2$														
		TED	AKX	AKX6	OLS6	LAS	ALAS	RID	ARID	ELA	AELA	SCA	ASCA	BAY	DAN	ADAN
whole	12.0	0.490	0.324	0.086	0.216	0.474	0.555	0.570	0.572	0.515	0.557	0.478	0.273	0.496	0.553	0.547
2013	7.9	0.590	0.333	0.050	0.194	0.550	0.696	0.716	0.718	0.621	0.703	0.557	0.270	0.654	0.695	0.696
2014	8.8	0.475	0.291	0.062	0.193	0.461	0.552	0.565	0.569	0.505	0.554	0.465	0.248	0.491	0.549	0.544
2015	10.2	0.532	0.361	0.094	0.247	0.516	0.593	0.603	0.609	0.548	0.596	0.525	0.348	0.529	0.588	0.585
2016	10.0	0.529	0.337	0.087	0.226	0.499	0.584	0.598	0.600	0.540	0.585	0.508	0.332	0.510	0.582	0.578
2017	5.5	0.402	0.224	0.026	0.149	0.395	0.472	0.490	0.492	0.434	0.475	0.396	0.229	0.431	0.470	0.467
2018	13.0	0.545	0.406	0.142	0.278	0.526	0.590	0.609	0.608	0.560	0.593	0.528	0.313	0.534	0.591	0.584
2019	9.1	0.468	0.304	0.069	0.205	0.454	0.524	0.541	0.542	0.493	0.525	0.457	0.249	0.470	0.523	0.514
2020	22.8	0.377	0.334	0.155	0.236	0.390	0.426	0.441	0.440	0.413	0.424	0.385	0.193	0.348	0.426	0.408

Period	RV (%)	Out-of-sample $R^2$														
		TED	AKX	AKX6	OLS6	LAS	ALAS	RID	ARID	ELA	AELA	SCA	ASCA	BAY	DAN	ADAN
whole	12.0	0.449	0.301	0.079	0.209	0.442	0.439	0.463	0.449	0.465	0.422	0.442	0.260	0.343	0.438	0.384
2013	7.9	0.546	0.316	0.049	0.193	0.514	0.597	0.614	0.610	0.570	0.589	0.515	0.261	0.511	0.596	0.571
2014	8.8	0.437	0.275	0.057	0.192	0.434	0.434	0.455	0.448	0.458	0.422	0.437	0.244	0.357	0.430	0.391
2015	10.2	0.499	0.349	0.091	0.252	0.492	0.492	0.500	0.487	0.511	0.471	0.497	0.333	0.361	0.480	0.413
2016	10.0	0.478	0.311	0.081	0.212	0.456	0.472	0.483	0.472	0.482	0.455	0.460	0.312	0.355	0.460	0.425
2017	5.5	0.367	0.202	0.024	0.144	0.361	0.341	0.379	0.362	0.383	0.323	0.359	0.220	0.253	0.341	0.283
2018	13.0	0.513	0.379	0.125	0.269	0.503	0.509	0.520	0.517	0.525	0.495	0.506	0.306	0.433	0.509	0.465
2019	9.1	0.421	0.282	0.070	0.195	0.407	0.388	0.430	0.407	0.428	0.372	0.403	0.223	0.301	0.400	0.338
2020	22.8	0.344	0.310	0.141	0.229	0.369	0.307	0.351	0.320	0.377	0.283	0.354	0.191	0.218	0.315	0.230

for the 10- and 30-min sampling frequencies, respectively. From Tables 2, 6, and 7, we find that the TED estimator consistently shows improved performance as the sampling frequency becomes higher. In contrast, the performance gains from using higher-frequency data are

Table 7: The annual average in-sample and out-of-sample  $R^2$  for the TED, AKX, AKX6, and various regression estimators across the five assets using 30-min sampling frequency data.

Period	RV (%)	In-sample $R^2$														
		TED	AKX	AKX6	OLS6	LAS	ALAS	RID	ARID	ELA	AELA	SCA	ASCA	BAY	DAN	ADAN
whole	12.0	0.438	0.321	0.115	0.218	0.474	0.519	0.535	0.536	0.502	0.518	0.474	0.233	0.470	0.511	0.507
2013	7.9	0.505	0.331	0.076	0.194	0.549	0.656	0.679	0.685	0.603	0.663	0.550	0.241	0.599	0.647	0.648
2014	8.8	0.419	0.294	0.088	0.195	0.462	0.510	0.530	0.529	0.495	0.510	0.466	0.210	0.460	0.503	0.499
2015	10.2	0.486	0.357	0.131	0.250	0.514	0.556	0.564	0.573	0.536	0.557	0.522	0.284	0.509	0.551	0.541
2016	10.0	0.459	0.330	0.115	0.226	0.498	0.549	0.562	0.568	0.527	0.550	0.501	0.282	0.497	0.538	0.535
2017	5.5	0.362	0.228	0.042	0.150	0.395	0.437	0.457	0.456	0.423	0.434	0.393	0.214	0.392	0.431	0.425
2018	13.0	0.496	0.402	0.183	0.280	0.529	0.566	0.578	0.581	0.554	0.566	0.529	0.238	0.504	0.562	0.556
2019	9.1	0.425	0.306	0.100	0.210	0.455	0.494	0.506	0.509	0.482	0.491	0.456	0.195	0.442	0.482	0.482
2020	22.8	0.355	0.321	0.187	0.234	0.388	0.382	0.399	0.391	0.398	0.374	0.373	0.205	0.354	0.377	0.369
Period	RV (%)	Out-of-sample $R^2$														
		TED	AKX	AKX6	OLS6	LAS	ALAS	RID	ARID	ELA	AELA	SCA	ASCA	BAY	DAN	ADAN
whole	12.0	0.404	0.301	0.107	0.211	0.440	0.416	0.448	0.430	0.454	0.401	0.437	0.226	0.380	0.419	0.393
2013	7.9	0.467	0.315	0.074	0.192	0.508	0.556	0.590	0.584	0.546	0.553	0.500	0.224	0.521	0.545	0.537
2014	8.8	0.391	0.278	0.083	0.194	0.429	0.405	0.443	0.424	0.440	0.392	0.430	0.208	0.370	0.404	0.392
2015	10.2	0.461	0.348	0.130	0.257	0.487	0.451	0.474	0.453	0.497	0.439	0.490	0.284	0.412	0.458	0.420
2016	10.0	0.418	0.308	0.109	0.213	0.459	0.435	0.466	0.445	0.472	0.424	0.462	0.275	0.385	0.429	0.404
2017	5.5	0.332	0.205	0.038	0.144	0.363	0.341	0.379	0.360	0.376	0.322	0.357	0.208	0.288	0.344	0.317
2018	13.0	0.467	0.378	0.164	0.271	0.506	0.491	0.507	0.502	0.519	0.483	0.508	0.233	0.443	0.503	0.465
2019	9.1	0.378	0.282	0.098	0.200	0.410	0.397	0.420	0.407	0.425	0.384	0.398	0.179	0.359	0.397	0.379
2020	22.8	0.332	0.304	0.173	0.231	0.368	0.284	0.331	0.297	0.369	0.248	0.344	0.205	0.289	0.294	0.267

relatively smaller for the benchmarks. This may be because the TED estimator captures the time-varying structure more effectively as the sampling interval becomes shorter, while the benchmarks fail to adequately account for this time-varying behavior.

In financial practice, the six factors (the Fama-French five factors and the momentum factor) are among the most frequently used canonical asset pricing factors. Thus, we investigate their integrated coefficient behaviors. Figure 9 depicts the estimates of the monthly integrated coefficients for the widely used MKT, HML, SMB, RMW, CMA, and MOM factors. We find that these factors are generally not significant for most periods and assets. This may be because the industry factors dominate the explanatory power of the six factors.



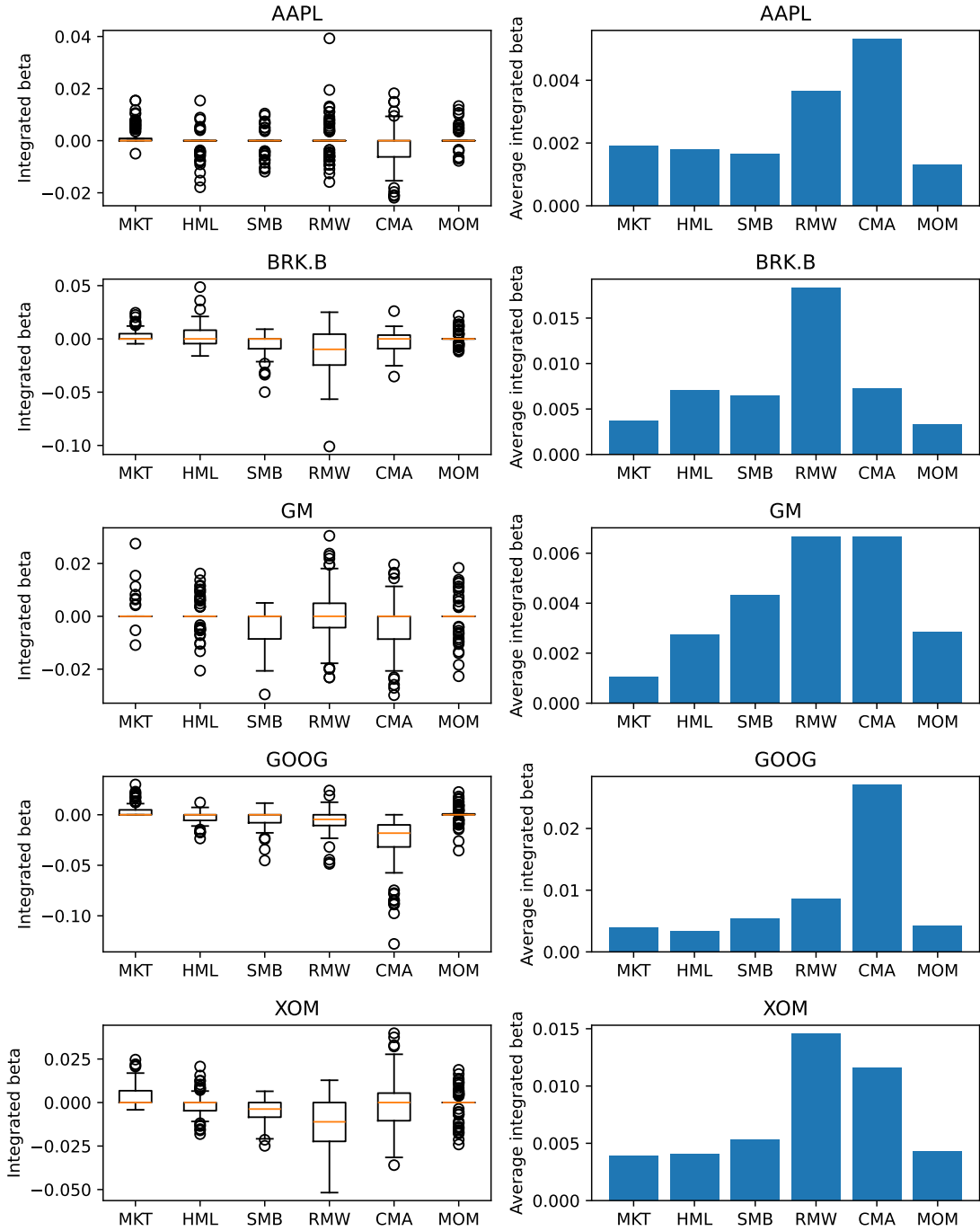


Figure 9: Boxplots of the integrated coefficient estimates from the TED estimation procedure (left) and the average  $\ell_1$ -norm (right) for the six factors, MKT, HML, SMB, RMW, CMA, and MOM.

## G Notation table

Table 8: Definitions of notations.

Notation	Meaning
$p$	dimension of covariate process
$n$	number of high-frequency observations
$Y_t$	dependent process
$\mathbf{X}_t$	$p$ -dimensional covariate process
$\boldsymbol{\beta}_t$	time-varying coefficient process
$Z_t$	residual process
$\boldsymbol{\mu}_t$	drift process of $\mathbf{X}_t$
$\boldsymbol{\sigma}_t$	volatility matrix process of $\mathbf{X}_t$
$\boldsymbol{\Sigma}_t$	instantaneous covariance, $\boldsymbol{\sigma}_t \boldsymbol{\sigma}_t^\top$
$\boldsymbol{\Sigma}_{XY,t}$	instantaneous cross-covariance, $\frac{d}{dt}[\mathbf{X}, Y]_t$
$\nu_t$	volatility process of $Z_t$
$\mathbf{B}_t, W_t$	standard Brownian motions of $\mathbf{X}_t$ and $Z_t$
$\boldsymbol{\mu}_{\beta,t}, \boldsymbol{\nu}_{\beta,t}$	drift and diffusion processes of $\boldsymbol{\beta}_t$
$s_p$	sparsity level (number of nonzero coefficients)
$\Delta_i^n A$	increment $A_{i\Delta_n} - A_{(i-1)\Delta_n}$
$\Delta_n$	sampling interval
$k_n$	window size (observations per time-localized window)
$\lambda_n$	tuning parameter for time-localized Dantzig selector
$\tau_n$	tuning parameter for time-localized CLIME estimator
$h_n$	thresholding level
$\widehat{\boldsymbol{\beta}}_{i\Delta_n}$	time-localized Dantzig selector
$\widetilde{\boldsymbol{\beta}}_{i\Delta_n}$	debiased instantaneous coefficient estimator
$\widehat{\boldsymbol{\Omega}}_{i\Delta_n}$	time-localized CLIME estimator
$I\boldsymbol{\beta}$	integrated coefficient
$\widehat{I\boldsymbol{\beta}}$	estimator of integrated coefficient before thresholding
$\widetilde{I\boldsymbol{\beta}}$	TED estimator
$s(\cdot)$	thresholding function
$\delta, q$	exponent in sparsity condition for $\boldsymbol{\beta}_t$ and $\boldsymbol{\Omega}_t$